Master's Thesis – Master Sustainable Development
Transmission Solutions for Floating Photovoltaics with Offshore Wind Energy in the North Sea - A Techno-Economic Analysis

Thomas Rogan (9450513)
Sustainable Development, Energy and Materials
Supervision by Dr. Sara Mirbagheri Golroodbari
Word Count: 18106
Date: 10-07-2023
30 ECTS

Acknowledgements

Throughout the journey of this master's thesis, I am grateful for the immense support and guidance I have received during the research and writing of this thesis. Firstly, I would like to extend my heartfelt thanks to my supervisor, Dr. Sara Mirbagheri Golroodbari. Sara's knowledge and expertise have been invaluable in providing continuous assistance and feedback on my topic. A special thank you goes to my parents and brothers, whose unwavering support made it possible for me to pursue my master's in Europe. Their belief in me and constant encouragement have been the driving force behind my achievements. Lastly, I want to express my deep appreciation to my friends, who provided me with support, ideas, and advice throughout this journey. Their presence and support were a constant source of strength and inspiration.

Summary

The transition towards renewable energy sources in the Netherlands has been by the need to meet future energy demands while addressing challenges such as limited land availability and competition for land use. Offshore wind and floating photovoltaics (FPV) present opportunities to address these challenges for renewable energy development. The rapid growth of wind farms in the North Sea in the coming decade, however, results in underutilized transmission capacity due to intermittence and wake losses within the wind farm. To optimize electricity generation and reduce costs, FPV can be combined with offshore wind to maximize the transmission capacity of substations and cables. Nonetheless, with high variability of solar and wind power production and problems with grid integration and congestion, green hydrogen emerges as a potential alternative cost-efficient transmission solution that can contribute to the Netherlands' renewable energy goals. Through examining these various transmission options, this research conducted a techno-economic analysis to determine the optimal method for energy transmission from offshore FPV integrated with offshore wind, while maximizing generation and transmission efficiency and minimizing costs. This research provides insights into the viability and limitations of transmission methods and explores the economic and market dynamics associated with offshore renewable energy transmission systems. The research identified the 2 GW HVDC VSC (High Voltage Direct Current Voltage Source Converter) transmission system as the best cost-efficient method for transporting energy from offshore wind and FPV. However, the integration of wind and FPV farms in a hybrid offshore system increases the curtailment of both sources, resulting in higher energy losses. The findings demonstrate that the integration of a hydrogen production plant can effectively increase the capacity factor of the hybrid system by converting excess energy into hydrogen, but this integration comes with additional costs. Advancements in hydrogen technologies and changes in the market may make the hydrogen production plant and pipeline a more viable and cost-efficient option in the future. It is recommended to explore all available options to enhance energy security and stability, even if it incurs higher costs, as the benefits of increased energy security could outweigh the financial implications, ensuring a more reliable energy system.

Table of Contents

1. Introduction

The fast-growing need to transition the energy sector towards renewable energy sources to meet the European Union (EU) climate targets has led to extensive growth of renewable energy development over the past decade in the Netherlands (IEA, 2021). Future scenarios to achieve climate neutrality by 2050 predict that electricity demand will grow from 110 TWh now to between 300 – 500 TWh in 2050 with the expectation 90% of electricity generation will come from renewable sources such as solar and wind (TNO, 2022). To meet this future demand and expected installed renewable energy generation, the Dutch government has constructed renewable energy road maps for solar photovoltaic (PV) and wind to achieve their targets. The solar PV systems and application roadmap targets to have a 200-gigawatt peak (GWp) of solar energy by 2050, currently at 2.8 GWp installed (Folkers et al., 2017, IEA, 2020). Although, the amount of land required for a solar farm depends on the technology used for the panel and the system. With a rough calculation, a solar farm need approximately $5000\ m^2$ for each MWp. Given, the limited land availability and increasing land prices in the Netherlands, floating photovoltaics (FPV) has emerged as a promising renewable technology for its ability to increase solar PV capacity in countries with land scarcity, while decreasing competition between renewables and land use practices, such as agriculture (CBS, 2021, SERIS, 2019). For this reason and having considerable access to water, the PV roadmap includes 24 GWp will be on inland waters and 45 GWp in the sea (Folkers et al., 2017).

In addition, a recent case study showed 80% of 20 FPV locations across the globe have a higher energy yield difference compared to ground-mounted PV, while other studies have shown FPV systems can mitigate water evaporation on water bodies prone to drought (SERIS, 2019, Golroodbari et al. 2023). However, a key disadvantage of offshore FPV systems is the higher capital investment as well as higher operation and maintenance costs compared to ground-mounted PV. In addition, offshore FPV systems are exposed to corrosion of electrical components from extreme weather conditions, wind and waves, and salt water, leading to more maintenance and a shorter lifetime (Sahu, 2016, Gorjian, 2021).

Recent research from the National Consortium Solar on Water, a Dutch consortium consisting of 32 governmental organizations and companies, is focused on developing large-scale FPV systems with the ability to endure serve weather conditions at sea. With the first 5 MWp expected to be built by 2026, the selected location for the construction is between wind turbines at the Hollandse Kust West wind farm in the North Sea (Dame, 2022). This allows FPV systems to generate energy in the unused

space at the designated wind farm zones while benefiting from the existing and planned substations and cables connected onshore. Due to the intermittence and wake losses in the wind farm, the maximum transmission capacity of the offshore substations and cables are underutilized as both are designed to transport the rated capacity, but the mean capacity of offshore wind is between 35-50% (Andrews and Jelley, 2022). A recent study showed that combining offshore FPV and wind farms could be a cost-efficient transmission solution to maximize the transmission capacity of the stations and cables to profit from more electricity generation and lower costs for electricity produced (Golroodbari et al, 2021). This is known as cable pooling.

Currently, the Netherlands wind roadmap plans is to have a total installed offshore wind capacity of 21 gigawatts in the North Sea by 2030 and connected onshore, dependent on distance and size, via either a 700 MW AC (alternative current) offshore substation or a 2 GW offshore AC/DC (direct current) converter station. The transmission system operator (TSO), TenneT is responsible for implementing and operating the offshore substation to support the transmission of offshore wind energy. The company currently operates four 700 MW AC offshore substations with plans to construct five more by 2026 in the North Sea. In addition, there are plans to construct at least fourteen 2 GW HVDC VSC stations by 2030 to connect green energy including further wind farms with large installed capacity (TenneT, 2022). The authors of the wind roadmap acknowledge that stations and cables capacity is only partly used, but it does not mention a hybrid wind farm with FPV and recommends overplanting wind turbines to increase the installed capacity (RVO, 2022). Combining FPV systems and wind farms could possibly be a preferable design as it maximizes the designated zones for wind farms without expansion, and also solar irradiance and wind speed have a negative correlation producing higher efficiency using the cable (Golroodbari et al, 2021). Still, solar and wind power production has high variability, leading to an imbalance in the electrical grid, and the combination of offshore wind and solar with onshore renewables can create periods of surplus electricity. Furthermore, the integration of large offshore renewable energy farms can be hindered by grid congestion, costing billions of euros to upgrade and reinforce the electricity grid (Weichenhain et al, 2019). Therefore, another alternative cost-efficient transmission solution could be green hydrogen, also known as carbon-neutral hydrogen. The Netherlands is aiming to be the EU's hydrogen hub with the goal to install 3 to 4 GW of electrolyzer capacity by 2030 (Gigler et al., 2022). Green hydrogen is expected to have a significant role in the Dutch energy transition, especially, targeting the energy-dense transportation sectors such as aviation and shipping. Present natural gas infrastructure can be retrofitted to transport hydrogen across the Netherlands and neighboring countries (Findlay, 2020).

Finally, offshore wind energy is viewed as to be critical to achieving green hydrogen. Numerous studies on the integration of hydrogen with wind systems have demonstrated reduced curtailment and transmission losses with additional revenue during peak periods and ensuring energy security (Carton & Olabi, 2010, Taieb & Shaaban, 2019). The 2030 wind roadmap considered green hydrogen as a transmission solution, but it was proven to be unrealistic due to high costs and low technological readiness.

This report will consider the potential development of offshore FPV that is integrated with offshore wind, and the crucial role of offshore renewables in accessing green hydrogen. To date, there have been no studies done on the energetic and economic effects of combining offshore wind with FPV on the planned substation and cables. As well as alternatively the effects of transmitting offshore wind and FPV by converting to green hydrogen have also not been assessed. Thus, a techno-economic analysis of transmission solutions for combined offshore and FPV farms will be completed.

A. Research Objective and Research Questions

In this research, the main objective is to present a techno-economic analysis to determine the optimal method to transmit energy from offshore FPV in combination with offshore wind to maximize the generation and transmission efficiency and minimize costs considering the planned designs for electrical transmission infrastructure. In addition, green hydrogen-based transmission infrastructure and hybridization of electricity and hydrogen design will be examined as an alternative based on market price and load management. This leads to the main research question and sub-questions:

How can we address the energy transmission for a hybrid offshore wind and floating solar PV system in a cost-efficient manner?

Sub Question:

1. What are the main components, designs, and technologies used with offshore electrical transmission infrastructure and what are their technical limitations?

2. What role can green hydrogen play as an alternative transmission solution, and how will the hydrogen market affect it as a viable alternative?

3. How does the levelized cost of electricity compare between different scenarios and operation modes?

B. Scientific and Society Relevance

The scientific and societal relevance of this research is to provide a cost-efficient method that maximizes the generation and transmission capacity of the offshore renewables and transmission methods, while benefiting society with affordable renewable energy. Scientifically, the research will address the existing knowledge gap in transmission efficiency and costs associated with combining offshore FPV and wind energy. As future roadmaps and tenders for offshore wind farms are expected to incorporate FPV, this research will give insight into the viability and limitations of the transmission methods under consideration. By identifying the specific factors that may impact the viability of each transmission method, this research can help optimize their utilization and identify areas for improvement. Additionally, green hydrogen production is also expected to be incorporated into these tenders to enhance the overall capacity factor. The exploration of green hydrogen as a transmission method aligns with the Dutch government and society's interest in hydrogen as a clean and sustainable energy carrier. Therefore, green hydrogen should be explored as a potential method of energy transmission. Furthermore, the societal relevance of this research will examine the economic and market value of each transmission solution to provide the lowest cost of energy to society. With the renewable energy sector undergoing rapid evolution in the coming decade, this research will examine the economic and market dynamics that influence economic feasibility and potential societal benefit of the considered transmission methods. Overall, this research will contribute valuable knowledge toward the advancement and implementation of offshore renewable energy transmission systems.

2. Methodology

This chapter provides an overview of the methods and equations utilized in this research. First, a literature review and semi-structured interviews were completed. After, an energy and cost model are developed for assessing mean energy production, energy transmission losses, lifetime production, and associated costs for combined wind and FPV farms within various transmission solutions in the North Sea. The modeling process employed widely used software such as Python and Excel. Furthermore, key information about the design, performance, and expenditures of the central transmission infrastructure and hydrogen transmission solutions are determined through a combination of literature review and semi-structured interviews. These factors are critical for calculating the annual mean production, annual transmission energy losses, and lifetime energy production as well as the total investment and operational and maintenance costs associated with each scenario. Additionally, the market and prices for electricity and hydrogen in Europe are examined to provide context for the analysis. Lastly, the four primary transmission methods for the scenarios are described: 700 MW HVAC, 2 GW HVDC, 650 MW hydrogen production plant and pipeline, and a hybrid approach combining the 2 GW transmission and 650 MW hydrogen production plant.

A. Literature Review

A literature review was conducted to obtain background information on the technical and economic characteristics of offshore renewables and hydrogen. The literature review gathered relevant scientific articles from search engines, such as, Google Scholar and ResearchGate, focusing on topics related to each sub question. Additionally, data and literature from governmental institutions and key stakeholders in the offshore wind, FPV, and hydrogen industries were collected. The identified papers and materials were thoroughly examined to extract valuable methods and information that could address the sub-questions. These insights were then used to develop the energy and cost modeling methodologies and to formulate semi-structured interview questions.

B. Semi-Structured Interviews

Semi-structured interviews were conducted to gather primary knowledge and information on the present technical and economic advancements within the previously mentioned industries (Kallio et al, 2016). The interviewees consisted of experts and companies involved in offshore renewables, systems

integration, and green hydrogen. These individuals and organizations were identified through the literature review and connection with my thesis supervisor. A total of 12 experts and companies were contacted via email, where the research of my thesis was explained, and sought their permission to participate adhering to Utrecht University's ethical guidelines. Ultimately, six interviews were conducted using MS Teams, following a semi-structured interview guide. The guide comprised 7-8 open-ended questions tailored to the expertise and background of each expert. The interviews were analyzed through a coding process, where relevant information was identified to further address the sub-questions. Transcripts of the interviews, along with the interview guide, can be accessed in the Appendix through a provided Google Drive link (Appendix A).

C. Energy Model

Site Description

The selection of the Doordewind Wind Farm Zone (DWFZ) Site I & II, for techno-economic analysis was based on its strategic location. It is in close proximity to the Ten noorden van de Waddeneilanden Wind Farm Zone (TWFZ) Site I, a 700 MW site, and Eemshaven, a vital natural gas hub in the Netherlands that has attracted green hydrogen projects from energy developers such as Shell and RWE. (RWE, 2022, Gasunie, 2020). The DWFZ is situated approximately 77 kilometers (km) off the coast of the Netherlands, approximate coordinates 54.248° N, 5.62° E. It covers an approximate area of 400 km^2 and has a total rated capacity of 4 GW. In an effort to simplify the calculations, the desired approach is to reduce the scale from 4 GW to one site of 2 GW for transmission restrictions. The tender process for the DWFZ is scheduled for 2027, and it is expected to be commissioned by 2031 (RVO, 2022). Figure 1 shows that the cable routes for the project are still being investigated.

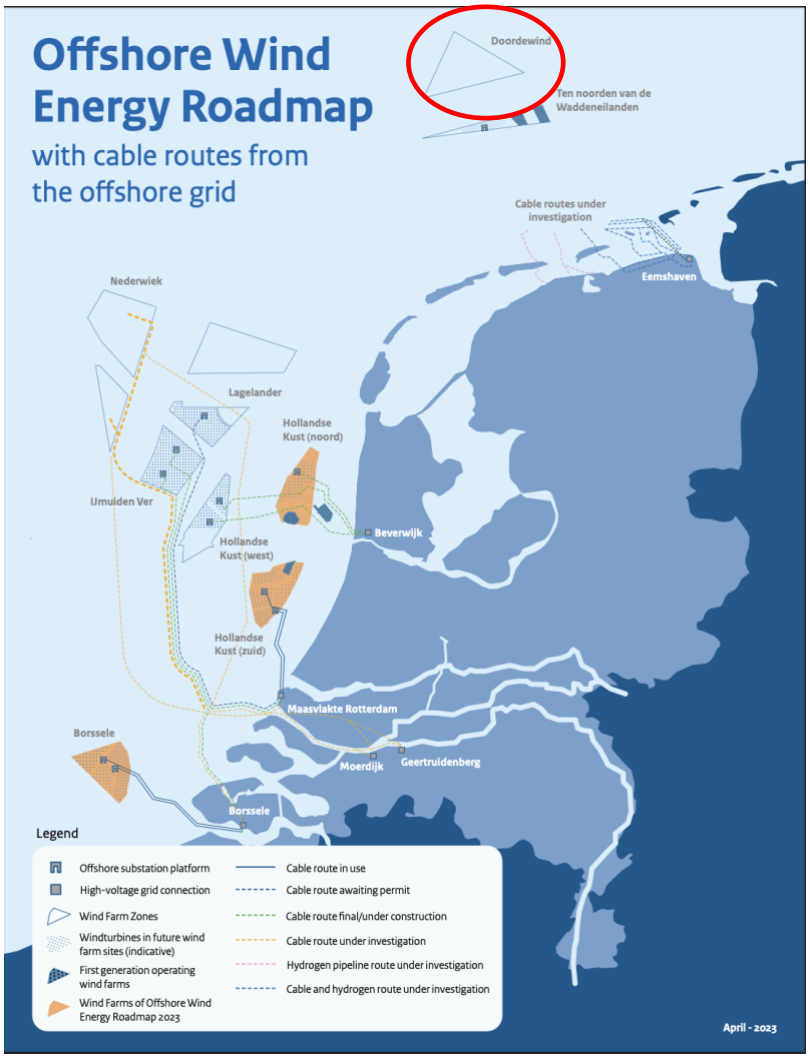

Fig 1: Planned and under investigation cable and hydrogen routes for offshore wind farms (Noordzeeloket, 2023)

Meteorological Data

The wind data was sourced from the KNMI North Sea Wind Atlas, which has reconstructed historical wind data, will be represented by u in this thesis, in the North Sea spanning from 1979 to 2014 (Wijnant et al., 2016). The dataset provides validated hourly wind speeds at various heights above sea level, ranging from 10 meters to 200 meters, on a 2.5 km^2 grid cell. For this analysis, the wind speed was considered at the hub height of 150 meters.

As for the solar data, it was sourced from the NASA Prediction of Worldwide Energy Resources (POWER) Project (NASA, 2023). This database contains historical hourly solar radiation data, $irr_{(h)}$, from 1981 to the present, measured in Wh/m^2.The solar data coordinates was chosen based on the location of the DWFZ.

In order to establish a base year, the wind and solar data from 2005 to 2014 were compared. Figure 2 displays that the year 2013 exhibited the closest average values, hence making it the most suitable base year for the analysis.

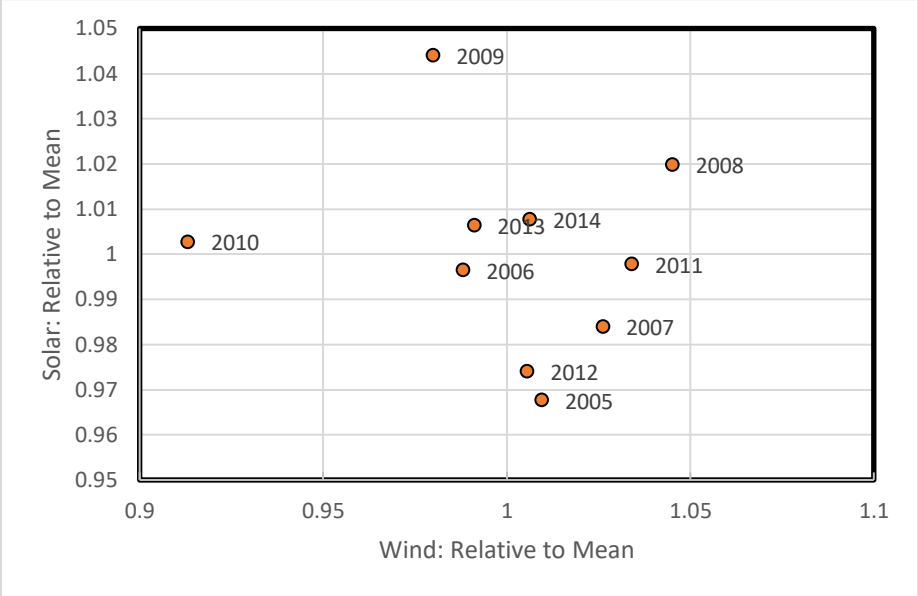

Fig 2: Scatterplot of solar and wind comparing the mean of annual solar irradiance ($kWh/m^2/yr$) and average annual wind speed (m/s) for 2005-2014.

Wind Turbine and Wind Energy Production

For the scenarios considered in this analysis, the reference offshore wind turbine is the fixed bottom-mounted Vestas V236-15.0 MW (Vestas Wind, 2023, Appendix B). Future projections suggest the utilization of a 15 MW turbine for the next wind farm tender in the Netherlands, known as IJmuiden Ver. Additionally, the V236-15.0 MW wind turbine is currently being deployed at a German wind farm in the North Sea (WWW, 2023, Knol & Coolen, 2019). The Vestas V236-15.0 MW is characterized by a theoretical power curve that includes a cut-in speed of 3 m/s, a cut-out speed of 31 m/s, and a rated power wind speed of 9.88 m/s, as depicted in Figure 3. This data is utilized to calculate these

production outputs: annual mean energy production, annual transmission energy losses, and lifetime energy production.

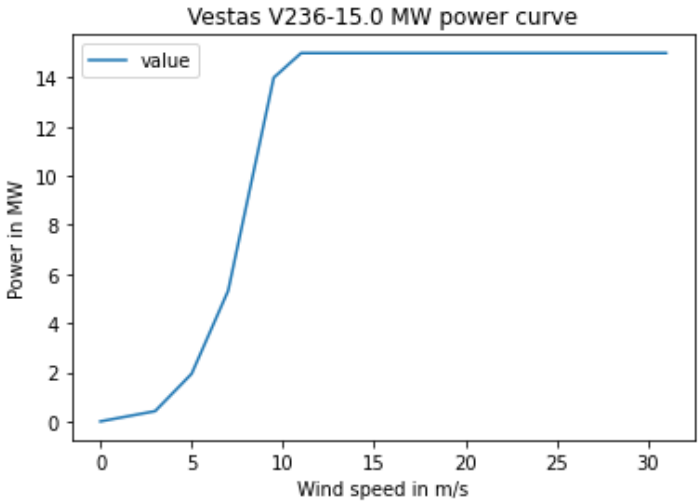

Fig 3: Theoretical Power Curve of Vestas V236-15.0 MW

The equations used to determine the potential hourly energy generation from the wind and FPV farm are explained by Golroodbari et al. (2021) and Andrews and Jelley (2022). First, the hourly wind speed data from the base year (which is shown as the year 2013) is utilized. Additionally, the maximum tip speed of 95 m/s, derived from a 15 MW wind turbine case study conducted by the National Renewable Energy Laboratory, is considered (Gaertner et al. 2020). Equation 1 is to calculate the hourly tip speed ratio, λ, with the previously mentioned data. Next, equation 2 is utilized to determine the hourly power coefficient, C_P, of the wind turbine. For a modern wind turbine, the value of K is approximately 100, and C_{PBetz} is equal to 16/27.

$$\lambda = \frac{V_{tip}}{u} \tag{1}$$

$$C_P \approx \left[\frac{\left(1-\frac{\lambda}{K}\right)}{\left(1+\frac{5}{\lambda^2}\right)}\right] C_{PBetz} \tag{2}$$

Where V_{tip} is a maximum tip speed [meter/second]
u is the hourly wind speed for 2006 [meter/second]
λ is the tip speed ratio [%]
K is the lift-to-drag ratio

C_{PBetz} is Betz Limit [%]
C_P is power coefficient of the wind turbine [%]

For a modern wind turbine, the value of K is approximately 100, and C_{PBetz} , Betz's coefficient, is a fundamental principle in fluid dynamics that describes the maximum possible efficiency for a wind turbine and is equal to 16/27. The power coefficient is a variable that quantifies the ratio of energy extracted by a wind turbine compared to the total energy available in the wind stream. As illustrated in Figure 4, the power coefficient as described in equations 2, has a non-linear relationship with wind speed.

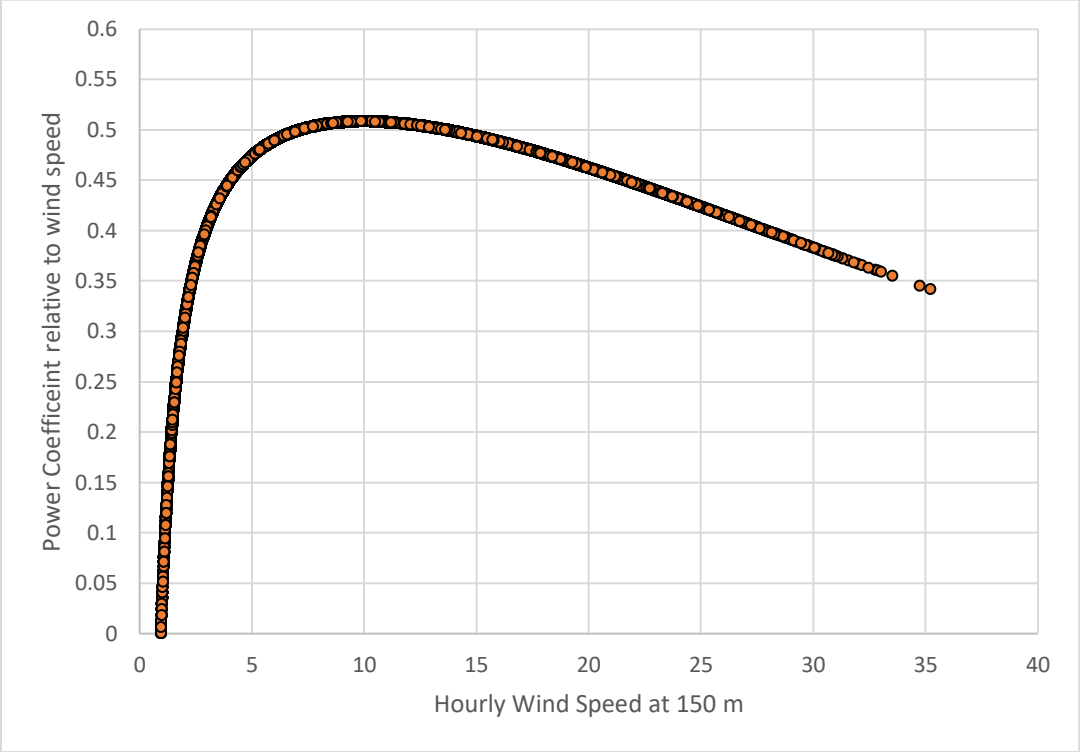

Fig 4: Scatterplot of solar and wind relating the power coefficient to hourly wind speed (m/s) for 2013.

To determine the mean energy production of a single wind turbine, equation 3 is utilized. Also, the Vestas V236-15.0 MW wind turbine has a swept area of 43,742 m^2, and the air density is considered fixed at 1.225 kg/m^3. By multiplying the hourly mean energy production by the number of wind turbines in each scenario, the annual mean energy production of the wind farm can be calculated using equation 4.

$$E_{WT_{(h)}} = \frac{1}{2}\rho A C_p u^3 \quad (3)$$

$$E_{WF_{(I)}} = N_{WT} * \sum E_{WT_{(h)}} \quad (4)$$

Where
ρ is the air density [kilograms/meter^3]
A is the area of the Vestas V236-15.0 MW [meter^2]
C_p is the power coefficient of the wind turbine [%]
$E_{WT_{(h)}}$ is the hourly mean energy output of a single wind turbine [Megawatts- hour]
N_{WT} is the number of wind turbines in the scenario
$E_{WF_{(I)}}$ is the annual energy output of the wind farm [Gigawatts-hours]

Solar Panels and Solar Energy Production

Since there are currently no commercial offshore FPV panels available with accessible technical specifications, the reference solar panels used for the scenarios have a maximum power point of 400 Wp or, η_{pv} , equal to 20.2%. (TCS, 2022, Appendix C). Each PV panel has an area of 1.98 m^2, A , meaning that a 1 MWp system would consist of 2500 panels and require an area of 0.00495 km^2. The energy production of the PV panels can be influenced by factors such as panel temperature and internal energy use from system components resulting in additional energy losses. To account for these losses, the performance ratio (PR) is implemented in the equation to represent the efficiency and effectiveness of the PV panels for converting solar energy into electrical power. The performance ratio is calculated by comparing the final PV yield to the reference yield (Reich et al., 2012). PR is a function of several metrics, and it may vary for different time intervals, for simplicity in this analysis, the averaged performance ratio of 85% was assumed in equation 5. The hourly mean energy production is then multiplied by the number of PV panels based on the size of the FPV farm in equation 6. This research ignores the shading effect of the PV panels from water, debris, and wind turbines.

$$E_{FPV_{(h)}} = A\,\eta_{pv}\,irr_{(h)}\,PR \quad (5)$$

$$E_{FPV_{(I)}} = N_{PV} * \sum E_{FPV_{(h)}}$$

(6)

Where A is the area of the PV panel [$meter^2$]
η_{pv} is the efficiency of the PV panel [%]
$irr_{(h)}$ is the solar irradiation per hour [Watt-hour/$meter^2$]
$E_{FPV_{(h)}}$ is the hourly mean energy output of the PV system [Megawatts- hour]
N_{PV} is the number of PV panels in the scenario
$E_{FPV_{(I)}} =$ is the annual energy production of the FPV farm [Gigawatts-hours]

Electrolyzer, Hydrogen Production Plant, and Pipeline (HPL)

The Nel Hydrogen MC 500 is the chosen reference electrolyzer for offshore hydrogen production scenarios (Nel, 2023, Appendix D). It possesses a rated capacity of 2.5 MW and yields a net production rate, NP, of 492 nm^3 or 44 kg of hydrogen per hour. In the case of a 100 MW plant, the overall lifetime efficiency, including the desalination unit and compressor, is assumed to be 6.1 kilowatt-hours (kWh) per nm^3, η_{Elec} ,(Hou et al. 2017). The 2.5 MW system, which includes the processing and transformer containers, requires an area of 61 m^2, thus a 100 MW plant would require 2.44 km^2. Although, if the containers were stacked on top of each other one time, that area requirement is halved. Using these specifications, it is determined that the maximum net production, MNP, of the electrolyzer reaches 19,680 nm^3 per 100 MW plant. Achieving this maximum net production necessitates a minimum of 121 MWh per 100 MW plant. The average energy production for hydrogen is then multiplied by the system size, denoted in terms of 100 MW, in equation 7 (Hou et al. 2017). One of the primary challenges with electrolyzers is cold starts, referring to when the electrolyzer initiates at a low temperature, resulting in poor efficiency and reduced hydrogen production. Usually, PEM electrolyzers provided a quick cold-start time, typically ranging from 10 to 20 minutes (Ansari, 2022). However, energy losses resulting from cold startups have not been taken into account.

$$E_{H_{(h)}} = \left(\frac{E_{FPV+Wind\ (I)}}{N_{Elec} \times NP \times \eta_{Elec}}\right) \times MNP \quad (7)$$

Where N_{Elec} is the number of electrolyzers per 650 MW plant
NP is the net production rate of the 2.5 MW electroylzer [nm^3 /hour]

MNP is the maximum net production rate of the 100 MW plant [nm^3 /hour]
η_{Elec} is the efficiency of the electrolyzers system [kWh per nm^3]
$E_{FPV+Wind\ (I)}$ is the total energy production from eq 4 & 6

Capacity Factor

The capacity factor expresses the full load hours of energy production seen in eq. 7 (Golroodbari et al., 2021, Badgett et al., 2021).

$$CF = \frac{\text{Total Energy Production Output } (MWh)\ (nm^3/h)}{\text{Rated Energy Production } (MW/nm^3) * 365\ * 24} * 100\ \% \quad (7)$$

Mean Energy Production

Scenarios 1 & 2

The primary limitation in the first and second scenarios is determined by the maximum rated capacity of the energy transmission platform and cables. In scenario one, the energy transmission constraint for combining wind and solar energy production is assumed to be 700 MW, which translates to 700 MWh in hourly resolution. In scenario two, the constraint is set at 2 GW, equivalent to 2 GWh. The curtailment ratio of the FPV farm with the combined wind farm size is depicted in equations 8 and 9. This is the mean energy available onshore based solely on the maximum capacity of platforms and cables.

$$E_{Mean_{S:I}} = E_{FPV+Wind\ (I)} < 700\ for\ h: [1,8760] \quad (8)$$

$$E_{Mean_{S:II}} = E_{FPV+Wind\ (I)} < 2000\ for\ h: [1,8760] \quad (9)$$

Scenario 3

The primary limitation in this scenario is the pipeline size, which is 400 mm, or has a maximum volume flow rate of 120,000 nm^3per hour, specifically for pure hydrogen (Kuczynski et al. 2019). The wind and FPV data from the first scenario, the 700 MW HVAC system, will be applied in scenario 3. The hydrogen production plant, with a capacity of 650 MW, requires a minimum of 787 MWh of electricity per hour to operate at maximum net production for the conversion process of green hydrogen. This energy input would result in a maximum net production of 127,920 nm3 of hydrogen per hour. However, due to the capacity limitations of the hydrogen pipeline, hydrogen production is restricted to 120,000 nm3 per hour, ensuring efficient transportation and utilization of the produced hydrogen. Lastly, the Lower Heating Value (LHV) of hydrogen is 3 kWh/nm^3 to comprehensively assess the implications of converting electricity to hydrogen and back to electricity (CASFHPU, 2004). It indicates that for every cubic meter of hydrogen gas consumed, approximately 3 kilowatt-hours (kWh) of energy can be generated. The curtailment ratio of the hydrogen production plant is based on combining wind and FPV farms is depicted in equation 10. This is the mean hydrogen available onshore based solely on the maximum flow rate capacity of the pipeline. For the purposes of this analysis, it is assumed that there are no energy losses due to pipeline leakage.

$$E_{Mean_{S:III}} = \mathrm{E}_{\mathrm{H}_{(h)}} < 120{,}000\ \mathrm{nm3}\ for\ h\text{: } [1{,}8760] \tag{10}$$

Scenario 4

Scenario 4 represents a combination of scenarios 2 and 3, incorporating various elements from each. In this hybrid scenario, the electricity system operates with a priority to meet the overall cable capacity, ensuring a stable and reliable power supply. Excess electricity generated beyond the cable's capacity is directed towards hydrogen production, following the principles of scenario 3. However, in the hydrogen priority scenario, hydrogen production takes precedence, and if the flow rate capacity of the pipeline is reached, any additional excess energy is transmitted onshore through the cables in Scenario 2. The allocation of electricity for hydrogen production can be categorized as "hydrogen-priority" when the electrolyzers are given preference first, or "electricity-priority" when only the surplus electricity is utilized by the electrolyzers. The aim is to see if this combined approach offers flexibility and adaptability in utilizing excess electricity and accessing the expenditures of combining both transmission systems. Although, for the lifetime production in Scenario 4, transmission losses will not

be considered. Instead, the focus will be on the mean energy production reaching cable or pipeline capacity for both electricity priority and hydrogen priority.

Energy Transmission Losses

Scenarios 1 & 2

There are several factors that contribute to energy loss during transmission to the onshore electrical grid. Firstly, the wake effect, η_{Wk}, within the wind farm can generate turbulence, resulting in decreased wind speeds and overall reduce energy production. In the absence of a specific wind farm design, the average wake effect for the 700 MW and 2 GW wind farms is derived from van den Brink et al. 2020. This study showed the average wake loss efficiency for the HVAC farms zones to be 90.4% and 87.87% for the HVDC farms zones. Secondly, the efficiency of the PV inverter, η_{Inv}, is set at the maximum European efficiency of 98.8%, based on Sungrow's 250 kW String Inverter (Sungrow, 2020). Lastly, the efficiency of the inter-array grid, η_{IG}, is assumed to be 99.9945% (Singlitico et al., 2021). These factors are incorporated into equation 10, using the mean energy production calculated in equations 4 and 6.

$$E_{Loss(I)} = \left(\left(E_{FPV_{(I)}} * E_{Loss_{Inv}}\right) E_{Loss_{Intra}}\right) + \left(\left(E_{WF_{(I)}} * E_{Loss_{Wak}}\right) E_{Loss_{Intra}}\right) \quad (10)$$

Where $E_{FPV_{(I)}} =$ is the annual energy production of the FPV farm [Gigawatts-hours]
$E_{Loss_{Intra}}$ is the efficiency of the inverter [%]
$E_{Loss_{Inv}}$ is energy loss from the intra-array grid [%]
$E_{WF_{(I)}}$ is the annual wind farm energy output [Gigawatts-hours]
` $E_{Loss_{Wak}}$ is the wake effect of the wind farm [%]
$E_{Loss(I)}$ is the energy loss at the platforms [Gigawatts-hours]

Next, the remaining energy wind and solar energy is collected at the offshore platforms to be pooled together on shore via the submarine cables while still taking into account the maximum capacity factor of each system. For HVAC transmission, it is assumed that the energy losses are .0319 % per km, including energy loss at the substations in eq. 11, and for HVDC transmission it is assumed that the energy losses are .0456% per km, including energy loss at the conversion stations, in eq. 12 (Negra

et al., 2006). This is the mean energy production with energy losses to examine available energy onshore to be fed into the electrical grid as E_{Tot}.

$$E_{Loss_{S:I}} = E_{FPV+Wind\ (I)} * (E_{Loss_{HVAC}} * D) \quad (11)$$

Where $E_{FPV+Wind\ (I)}$ is the annual wind farm energy output after $E_{Loss(I)}$ [Gigawatts-hours]
$E_{Loss_{HVAC}}$ is the energy loss efficiency of the HVAC [%/km^2]
D is the distance [km^2]
$E_{Loss_{S:I}}$ is the energy loss from the platforms to the national electrical grid in Scenario 1[Gigawatts-hours]

$$E_{Loss_{S:II}} = E_{FPV+Wind\ (I)} * (E_{Loss_{HVDC}} * D) \quad (12)$$

Where $E_{FPV+Wind\ (I)}$ is the annual wind farm energy output after $E_{Loss(I)}$ [Gigawatts-hours
$E_{Loss_{HVDC}}$ is the energy loss efficiency of the HVDC [%/km^2]
D is the distance [km^2]
$E_{Loss_{S:II}}$is the energy loss from the platforms to the national electrical grid in Scenario 2[Gigawatts-hours]

Scenario 3

By utilizing the remaining wind and solar energy, as outlined in equation 10, the data is inputted into equation 7. This calculation allows for the determination of energy loss and the availability of hydrogen energy to be supplied to the national electricity grid onshore. Additionally, the process of converting hydrogen back to electricity, based on the LHV of hydrogen, will be demonstrated, providing insights into the efficiency of the hydrogen-to-electricity conversion process.

Lifetime Production

Scenarios 1, 2 & 3

The aging of machinery components is an undeniable reality that affects the efficiency and durability of various aspects of wind turbines and FPV systems. When the capacity factor of the wind farm and

solar panels decreases with age, it results in reduced cumulative lifetime energy output from wind and FPV farms. This decrease contributes to an increase in the levelized cost of electricity (LCOE) generated by wind and FPV farms. In cases where the rate of degradation is excessively high, it may become economically viable to replace the turbines and panels prematurely with newer models. Such premature replacements further contribute to higher costs associated with wind and FPV farms. Accurately quantifying the aging of these machinery components, or degradation rate, is important to making investing and decisions for key stakeholders and energy developers. According to the findings presented by Staffell and Green (2014), DWFZ Site wind farm is assumed to experience a degradation rate of 12% over a twenty-year lifespan (equivalent to 0.6% per year). While Jordan and Kurtz (2012) have reported in their finds, the efficiency of solar panels decreases by an average of 0.5 percent per year. Also, the annual degradation rate of 1% for the PEM electrolyzers is derived from Keddar et al (2022). Based on these assumptions, the calculation of the DWFZ wind farms, FPV farms, and hydrogen electrolyzer production plant energy production over 20-year lifetime is expressed in Equation 13, 14, and 15. These lifetime productions will used as $E_{FPV+Wind\,(II)}$ from Equation 10, 11, and 12 to understand the full energy loss over the lifetime. This is the total energy production with mean energy and energy losses available on shore to be fed into the national grid onshore.

$$E_{WF_{(LT)}} = \sum_{n=1}^{LT_{WF}} E_{WT_{(Mean)}} * (1 - .006)^{n-1} \tag{13}$$

$$E_{FPV_{(LT)}} = \sum_{n=1}^{LT_{FPV}} E_{FPV_{(Mean)}} * (1 - .005)^{n-1} \tag{14}$$

$$E_{H_{(LT)}} = \sum_{n=1}^{LT_{H}} E_{H_{(Mean)}} * (1 - .01)^{n-1} \tag{15}$$

Where $E_{WT_{(Base)}}$ is the wind farm energy generation in base year for 2013 [Gigawatts-hours]
$E_{FPV_{(Base)}}$ is the FPV farm energy generation in base year for 2013 [Gigawatts-hours]
$E_{WF_{(LT)}}$is the cumulative amount of energy generated by the wind farm [Gigawatts-hours]
$E_{WF_{(LT)}}$is the cumulative amount of energy generated by the wind farm [Gigawatts-hours]

LT_{WF} is the lifetime the wind farm is operational [years]
LT_{FPV} is the lifetime the FPV farm is operational [years]
n is the summation index

Scenario 4

As mentioned earlier, Scenario 4 combines elements from scenarios 2 and 3. In the electricity priority scenario, any surplus electricity is utilized for hydrogen production. Conversely, in the hydrogen priority scenario, excess electricity is redirected into the cables. This scenario considers the degradation rates of each energy generation source to gain a comprehensive understanding.

D. Cost Modeling

The purpose of the cost model is to determine the future benefits and the levelized costs associated with different scenarios by assessing the lifetime investment and operational costs and analyzing lifetime generation (Golroodbari et al. 2021, Andrews and Jelley, 2022). By utilizing this cost model, it becomes possible to estimate the overall cost efficiency and financial investment costs of various energy transmission scenarios. First, the future cash flows derived from the sale of electricity or hydrogen, the model provides insights into the profitability of each scenario, B, in equation 16 and 17. Secondly, the lifetime costs encompass expenses related to infrastructure, components, and installation in the base year,I_0, while the operational costs consider ongoing maintenance, repairs, and other expenditures, C_n , in equation 18. Also, it is assumed the interest rate is 3% and the annual lifetime of each scenario is 20 years in equation 18. After, the lifetime energy generation of each transmission solution will be applied in Equation 19. Finally, these results will be used to calculate the levelized costs over the lifetime production of each scenario in Equation 20.

Lifetime Benefit

$$B = E_{Tot_{ele,p}} P_p + E_{Tot_{ele,op}} P_{op} \tag{16}$$

$$B = E_{Tot_H} P_H \tag{17}$$

Where P_p is the peak price of electricity [€]
$E_{Tot_{ele,p}}$ is the electricity total for peak electricity [Gigawatts-hours]
P_{op} is the off-peak price of electricity [€]
$E_{Tot_{ele,op}}$ is the electricity total for off peak electricity [Gigawatts-hours]
P_H is the price of the green hydrogen [€]
B are profits from sold electricity or hydrogen [M€]

Lifetime Costs

$$\text{Life Time Costs } = I_0 + \sum_{n=1}^{Nyear} \frac{C_n}{(1+r)^n} \tag{18}$$

Lifetime Generation

$$Total\ Lifetime\ Energy\ Generation = \sum_{n=1}^{Nyear} \frac{E_{Tot_n}}{(1+r)^n} \tag{19}$$

Levelized Costs of Electricity/Hydrogen

$$LCOE/H = \frac{Life\ Time\ Costs}{Total\ Lifetime\ Energy\ Generation} \tag{20}$$

Where I_0 is the base year investment costs of the transmission system [€M]
C_n is the annual operation and maintenance costs [€M]
E_{Tot_n} is the total lifetime energy generation [Gigawatts-hours]
r is the interest rate [%]
n is the summation index
N_{year} is the number of years of operation [20 years]

E. Design, Performance, Expenditure

The following explains further in-depth the central electrical infrastructure components and hydrogen production components for this analysis.

Inverters

Design

One central infrastructure component of FPV farms is an inverter, which converts DC to AC to be usable in the electrical grid and assist in extracting the full energy production of the FPV farm (Vairavasundaram et al. 2021). The design chosen for the analysis is the string inverter compared to a centralized inverter as they benefit from having a multitude of MPPT and ensure the strings are being well managed to increase the energy output of the FPV farm (Interviewee 5, 08-05-23). Even though the shadow effect was not considered in this analysis, the string design layout of inverters can minimize a failure by only effects a small area of the FPV farm compared to the centralized (Muhammad et al., 2021). Typically, inland FPV systems have their inverters located onshore in a secure container structure to prevent environmental conditions from degrading the system and leading to further energy losses (Siemens, 2023). However, offshore FPV systems and inverters will be locations that endure more harsh weather conditions from waves, wind, and salt water. Therefore, to prevent energy losses and offshore environmental conditions, offshore inverters will ideally need to be located above sea level in a weather secured container on a floating barrage or platform (Interviewee 1, 31-03-23). Also, these containers can be equipped with a potential advanced water-cooling systems like immersion cooling that is currently used in data centers and bitcoin mining industries. In addition, the containers are preconstructed on land to facilitate their easy deployment in the ocean and to accommodate the scalability requirements for larger offshore FPV systems anticipated in the 2030s (Interviewee 1, 31-03-23). After the inverters, there is a low voltage switchgear and transformers to increase the voltage to reduce the energy losses in the PV cables. This is then fed into a central point for all the FPV energy to be transmitted to the offshore platforms (Interviewee 5, 08-05-23).

Performance

As mentioned before, the inverter being assumed in this analysis is Sungrow's 250 kW. In this analysis, the inverter used is the same type of model as the inverters for ground-mounted PV farms. Over the past decade, modern solar inverters have made significant advancements in terms of efficiency. Thanks to ongoing technological improvements, high-quality inverters now boast maximum rated efficiencies of up to 98%, as stated in manufacturers' data manuals (Shawn, 2013). Inverters commonly do not operate at their nominal rated efficiency and the inverter operating at a lower or higher power range can lead to lowered efficiencies. Thus, PV panels producing higher energy output ranges should be equipped with oversized inverters to reduce power loss and heating of the inverters. With very high solar irradiance occurring for short periods, oversized inverters can handle the maximum power flux compared to undersized inverters, which can reach their maximum power flux and convert less energy during those periods (Vignola, et al, 2004; Interviewee 5, 08-05-23). Also, the inverters require a minimum amount of energy to operate and low power ranges can generate lower efficiencies. These limitations related to the environment and location of the inverters are overcome by introducing software and monitoring provided by the inverter manufacturers to provide more accurate performance estimates over its lifetime (Kratzenberg et al. 2014). At present, there is a lack of available offshore FPV energy generation data with research, including the current analysis, relying on solar irradiation data from the location and does not incorporate the influence of environmental conditions on the outcomes (Interviewee 2, 06-04-23). Hence, it becomes challenging to accurately assess the overall efficiency of the inverters. Nevertheless, through strategic design and planning, it is possible to mitigate these factors that can contribute to lower efficiency rates.

Expenditure

The Sungrow SG 250 HX offers an investment opportunity for large-scale solar power projects with an investment cost of 4 million euros per 100 MWp, this includes the installation costs and weather secure containers (Ramasamy & Robert, 2021, Enbar et al., 2015). However, it is critical to consider the long-term operational aspects and costs associated with this technology. Given the offshore environment conditions for PV inverters, their performance gradually diminishes over time. Thus, it is anticipated that within 20 years, at least one replacement of the inverters will be necessary to maintain optimal efficiency and power output (SERIS, 2019, Interviewee 1, 31-03-23). This replacement cost must be factored into the overall financial considerations for deploying the Sungrow SG 250 HX. Furthermore, to ensure the operation of the inverters, annual maintenance is required. It is estimated

that the operation and maintenance costs will amount to approximately 1% of the total investment costs (Enbar et al., 2015). These expenses cover routine inspections, preventive maintenance, and any necessary repairs to guarantee consistent and reliable performance throughout the operational lifespan of the FPV farm.

HVAC & HVDC VSC and Cables

Design

The 700 MW HVAC platforms are currently in use, connecting smaller and closer to shore wind farms like Brossele Sites and Hollandse Kust Zuid, with a maximum rated transmission capacity of 700 MW. However, considering the higher load factor agreed upon with wind farm developers, the real rated capacity ranges from 700 MW to 760 MW, ensuring a guaranteed minimum transmission capacity of 700 MW. Each of the alternating current platforms is linked to the onshore high-voltage grid through a dual arrangement of two 220-kilovolt cables. This configuration enhances system availability, mitigating the risk of partial or complete disruption of transport capacity. Furthermore, the electrical setup on the wind turbine connection side is designed in a manner that allows for seamless switching of the wind farms to an alternative offshore transformer in the event of a failure in one of the 220-kilovolt cables or its associated transformers. This redundant setup ensures additional availability, ensuring that at least half of the transport capacity remains operational even in the face of such failures. These platforms consist of 16 usable J tubes, with each carrying a theoretical capacity of 60-70 MW, requiring 12 J tubes for connecting the wind farm (TenneT, 2016, RVO, 2022). Therefore, the remaining J tubes allow for an approximant maximum capacity of 300 MWp for the FPV farm.

As for the 2 GW HVDC VSC platform, they are currently under development and expected to be commercially available for further offshore wind farms like Ijmuiden Ver Sites and Nederwiek Sites. This platform will exhibit a maximum rated capacity of 2 GW, yet with the higher load factor agreed upon, the real rated capacity ranges from 2 GW to 2.3 GW, ensuring a guaranteed minimum transmission capacity of 2 GW (RVO, 2022). The new design incorporates four transformers within the platform, enabling the collection of energy from surrounding wind farms at a higher voltage. Additionally, our platform employs an advanced cooling system known as "oil natural air natural" (ONAN). The ONAN circulates the oil for the transformer through cooler banks located on the offshore platform where outside air can cool the system. By utilizing this type of cooling method, we have

reduced the need for auxiliary systems, maintenance requirements, and energy consumption. Moreover, the ONAN cooling system enhances the robustness of our transformers, as evidenced by its successful implementation on our 700 MW AC platforms off the Dutch shore. The newly developed cable system consists of four individual cables bundled together: a negative and positive 525 kV pole, a metallic return, and a fiber-optic cable. This advanced HVDC cable offers significantly higher capacity compared to HVAC, allowing for more efficient transmission over long distances while minimizing costs. Furthermore, it has a positive environmental impact by reducing the number of cables utilized for each wind farm. Similar to before, the new cable system ensures that it can continue operating at 50% capacity even in the event of cable failures (TenneT, 2023). The platforms will feature 28 usable J tubes to connect the wind farm and FPV farm, and assuming a minimum rated capacity of 15 MW for wind turbines, the maximum capacity for the FPV farm is estimated to be 500 MWp (RVO, 2022).

In both systems, the array cables connecting the wind farm and FPV utilize 66 kV cables. The utilization of 66kV array cables was chosen instead of 33kV cables as it reduces the costs by laying less cable and generally better transmission of larger wind turbines (Vis, 2020, RVO 2022). In each scenario, it is estimated that a single wind turbine would require approximately 1.47 kilometers of 66 kV cables. Similarly, for a 100 MWp FPV farm, it is assumed that approximately 10.29 kilometers of 66 kV cables would be needed to accommodate the 100 MWp capacity (van den Brink et al., 2020).

Performance

Lazaridis (2005) and Negra et al. (2006) present the percentage of transmission loss for a 700 MW and 1000 MW wind farm in both HVAC and HVDC VSC scenarios. In the HVAC transmission system, several key components contribute to energy loss when connecting large offshore wind farms. These include HVAC submarine transmission cables, offshore transformers, compensation units, thyristor-controlled reactors (TCR), and onshore transformers. In the case of a 700 MW HVAC system, the electricity is transmitted through four 220 kV cables, resulting in an energy loss of 0.0319 per kilometer. For the HVDC transmission system, connecting large offshore wind farms involves various components that contribute to energy loss. These components encompass the VSC (Voltage Source Converter) station circuit breaker, system-side harmonic filter, interface transformer, converter-side harmonic filter, VSC unit, VSC DC capacitor, DC harmonic filter, DC reactor, and DC submarine

cable. In the case of a 1000 MW HVDC system, through conversion station and cables, resulting in an energy loss of 0.0456 per kilometer. In HVAC systems, most of the energy loss takes place within the cables which is due to skin effect in AC cables, meanwhile, in HVDC systems, the primary source of energy loss is attributed to the offshore and onshore conversion stations. Finally, the energy loss in the inter-array grid is estimated to be approximately 0.55% of the total electric energy transmitted (Singlitico et al., 2021).

Expenditure

The expenditure for offshore HVDC VSC and HVAC transmission systems can vary depending on several factors (Lazaridis, 2005, Ruijgrok et al. 2019). HVDC systems are generally more expensive to install compared to HVAC systems due to their converter stations and required equipment. HVDC systems are preferred for long-distance transmission and interconnections between different power grids, as they offer lower transmission losses and higher capacity. However, the cost of laying submarine cables and constructing offshore and onshore converter stations for HVDC can be substantial. On the other hand, HVAC systems are typically more cost-effective for shorter distances and when connecting nearby offshore wind farms. The costs primarily involve laying submarine cables and installing offshore and onshore substations (Fernández-Guillamón et al. 2019). For a HVDC VSC, the annual operation and maintenance cost is estimated at 0.5% of the investment cost, while the annual operation and maintenance cost associated with HVAC equipment is assumed to be 0.75% of the investment costs (Van Eeckhout et al. 2009). The main components and their related costs are listed in table 1.

Table 1: Overview of the HVAC and HVDC VSC components and costs

Component	HVAC	HVDC VSC
700 MW & 2 GW Offshore Converter/Substation Costs (M€)	8	440
66 kV Inter array Cables & Installation Costs (M€/km)	.22	.22
220 kV HVAC & 525 kV HVDC Export Cable & Installation Costs (M€/km)	1.75	1.0
700 MW & 2 GW Onshore Converter/Substations Cost (M€)	8	440
Annual Operation and Maintenance Costs (M€)	4.7	10.0

Electrolyzer System and Pipeline

Design

Green hydrogen is produced through water electrolysis, splitting water into hydrogen and oxygen, which is powered by renewable electricity generation. The central component is an electrolyzer and two main electrolyzers are being used alkaline electrolyzer and proton exchange membrane (PEM) electrolyzers (DOE, 2022). The design chosen for this analysis is the PEM electroylzers as it offers several advantages, including rapid start-up, corrosion resistance, simplified maintenance, and fewer components compared to alkaline electrolyzers involved in the manufacturing (Grigoriev et al, 2014, Guo et al. 2019). Additionally, there have been notable advancements in increasing the stack capacity of this type of electrolyzer. In addition, PEM electrolyzers have a small footprint and require relatively less space, important for limited space on offshore platforms. High manufacturing costs are a major factor in restricting large scale development of PEM electrolyzers (Kumar & Himabindu, 2019). But potential future advancements in new catalysts and materials can increase the efficiency and provide cost effective green hydrogen on a large scale. In addition, the durability and lifespan of electrolyzer systems are expected to improve, reducing the frequency of replacement and maintenance (IRENA, 2022, Interviewee 3, 12-04-23). The 650 MW hydrogen electrolyzer production plant should be located offshore next to or on top of the offshore electrical platforms allowing for easier integration into the offshore renewables and lower energy transmission losses. Several important components need to be considered in the offshore hydrogen electrolyzer production plant besides the electrolyzer, namely the desalination unit and compressor. Offshore green hydrogen production generates three primary by-products: pure hydrogen, oxygen, and salt. Pure hydrogen can be compressed and transported through the pipeline infrastructure for various applications onshore. Additionally, the oxygen by-product can be compressed and utilized in other industries or processes (Iberdrola, 2021). However, the release of considerable quantities of salt resulting from the large volumes of water required for hydrogen production can have detrimental effects on the environment. This salt discharge can pose challenges during the permitting process, as uncertainties and potential ecological impacts are typically not favorable for wind farm tenders (Interviewee 2, 06-04-23, Interviewee 4, 26-04-23). Nevertheless, ongoing pilot projects aim to address and find solutions to these environmental concerns, providing valuable insights and data to inform future practices and mitigate potential impacts. Finally, future designs for electrolyzers show promising potential for integration within offshore turbines (Interviewee 4, 26-04-23). This approach is considered advantageous because it can be challenging to incorporate electrolyzers into offshore electrical systems that are planned years in advance (Interviewee 5, 08-05-

23, Interviewee 6, 09-05-23). By integrating electrolyzers directly into the turbines, there can be reduced energy losses through conversion between hydrogen production and offshore wind energy generation. This approach offers the opportunity to reduce space utilization and the system design, leading to enhanced efficiency and another potential cost-effective solution for integrating offshore hydrogen production.

When designing a pipeline, such as one with a diameter of 400 mm and a maximum volume flow rate of 120,000 nm^3 per hour, specifically for transporting pure hydrogen, several considerations are needed. Ensuring the appropriate selection of materials and implementing robust safety measures to prevent leakages and accidents are crucial aspects of pipeline design. Compliance with environmental and regulatory standards further supports these efforts (Interviewee 3, 12-04-23, Interviewee 4, 26-04-23). However, cost-effective solution to prevent hydrogen pipeline construction is by leveraging existing natural gas pipelines that can be retrofitted with minimal additional costs compared to constructing new HVDC or HVAC export cables and power lines. Retrofitting existing pipelines allows for the repurposing of infrastructure, reducing the need for extensive construction and installation. Also, utilizing hydrogen pipelines to transport energy helps alleviate grid congestion (Gigler et al., 2022). Diverting a large portion of energy transportation from the electrical grid to the hydrogen pipelines, the overall burden on the grid is reduced. By leveraging hydrogen pipelines as an alternative energy transportation infrastructure, the strain on the electrical grid can be mitigated and provide a more efficient and stable distribution of energy throughout the electrical grid (Interviewee 4, 26-04-23, Interviewee 6, 09-05-23).

Performance

As mentioned before, the PEM electrolyzer being used in this analysis is Nel Hydrogen MC 500. One of the primary issues with the PEM electrolyzer is the high energy consumption where it's assumed to have an average lifetime efficiency of 6.1 kWh per nm^3 and every nm^3 can produce 3 kWh (Hou et al. 2017). This indicates that over 50% of the energy utilized in the hydrogen production process is lost during the conversion. One crucial common strategy to improve the performance of the water splitting is enhancing the effectiveness of the electrocatalysts. The catalytic activity serves as a significant parameter for evaluating their effectiveness, while long-term stability is crucial for assessing the overall quality of electrocatalysts in water splitting (Chi & Yu, 2018, Wang et al., 2022).

However, the expensive costs of these precious metals used in the catalysts hinder their widespread practical application. Research focusing on electrocatalysts with fast start up times, long term durability, and low cost is necessary to increase overall energy efficiency and stability with the electrolyzer. By making progress in these areas, there can be larger scale commercial development and deployment of PEM water electrolysis technology at low costs (Chi & Yu, 2018, Wang et al., 2022).

Large, new gas hydrogen pipelines present a promising option for long-term cost-effective transmission compared to HVDC electric lines. A 36-inch diameter GH2 pipeline operating at 1,000 psi can continuously transmit approximately 6,000 MW of energy and provide a significant energy storage capacity of around 120 GWh (Keith & Leighty, 2002). An example of a major pipeline is the Balgzand Bacton Line (BBL), a 235-kilometer gas pipeline that facilitates the transportation of natural gas between the Netherlands and Great Britain. The pipeline has an approximate hourly capacity of 20 GW for gas flow, or 6,867,000 nm^3/h of hydrogen, from the Netherlands to Great Britain, and an hourly capacity of 7 GW for gas flow, or 2,333,000 nm^3/h of hydrogen, from Great Britain to the Netherlands (BBL Company, 2023, Interviewee 4, 26-04-23). It helps to enhance the supply security of Great Britain and the Netherlands, while facilitating the integration of the European gas market, and leveraging price differences between the gas markets. The high energy-carrying capability of gas pipelines makes them highly efficient for large-scale hydrogen transportation (Interviewee 4, 26-04-23). With construction and regular maintenance, steel pipelines exhibit long service lives. In the future, it could be beneficial for the energy industry to construct new natural gas transmission pipelines that can transport hydrogen also. This approach would enable a well-ordered transition, as these pipelines can initially transport a mixture of natural gas and hydrogen, gradually increasing the concentration of hydrogen until the pipeline is carrying 100% hydrogen (Mahajan et al 2022). Also, underground pipelines for transmission are generally better received by the public compared to overhead electric transmission (Keith & Leighty, 2002). While storage was not specifically addressed in this research, hydrogen production can be stored in large quantities at a low cost. This can be achieved by utilizing underground geological formations such as gas fields and salt caverns, which provide suitable storage options for hydrogen (Caglayan et al, 2020, Interviewee 4, 26-04-23). These formations offer the potential for secure and efficient storage of hydrogen, ensuring its availability when needed for various applications.

Expenditure

The expenditures associated with PEM water electrolyzers can vary depending on various factors. The primary cost components include materials, manufacturing processes, system design and installation, and operational expenses. The electrolysis system and hydrogen pipeline and associated installation costs are shown in Table 2. The annual operation and maintenance costs are assumed to be 2% of the investment of the investment costs. This includes PEM electrolyzers requiring the replacement of stakes once in their lifetime to ensure their continued efficient performance (Christensen, 2020, Breunis, 2021).

Table 2: Overview of the Hydrogen production components and costs

Component	Elec + HPL
Electrolyzer System & Installation Costs (€/kW)	1065
66 kV Inter array Cables & Installation Costs (M€/km)	.22
400 mm Hydrogen Pipeline & Installation Costs (M€/km)	1.0
Annual Operation and Maintenance Costs (M€)	16.79

F. Electricity and Hydrogen Market

Electricity Market and Price

Given the complexity of the energy market system and, throughout the year, the price of electricity exhibits a seasonal dependency, reflecting variations in consumption and production levels. The Amsterdam Power Exchange (APX), now integrated into the European Power Exchange (EPEX), represents the price at which energy suppliers can sell a given quantity of electricity. Typically, energy modeling systems utilize the day-ahead price, which is determined based on historical and current demand data. The APX market categorizes energy prices into two distinct types: peak prices, applicable from 8 am to 8 pm, and off-peak prices, from 8 pm to 8 am. The expansion of installed renewable energy sources is anticipated to lead to a higher occurrence of negative electricity prices. With the possibility for negative electricity prices to occur more frequently, hydrogen production and storage can be seen as an opportunity to underscore these negative prices. To simplify the representation of future energy prices and account for the inherent uncertainty in forecasting, the average annual price of electricity is 50 €MWh for peak prices, P_p, and 40 €MWh for off-peak prices, P_{op} (Golroodbari et al. 2021).

Hydrogen Market and Price

The market and pricing of hydrogen in the Netherlands and Europe hold significant potential as countries strive to transition towards a low-carbon economy. As the demand for clean energy and decarbonization efforts continue to grow, green hydrogen is increasingly seen as a crucial element in achieving renewable energy targets (EU Commission, 2023). Green hydrogen is recognized as a key solution for decarbonizing energy-intensive industries like aviation, shipping, and steel manufacturing. However, it can be primarily regarded as a versatile method to transport, store, and utilize inexpensive renewable energy during periods of high demand (Interviewee 4, 26-04-23). This capability addresses the intermittent nature of offshore wind and FPV by converting excess energy into hydrogen for later use. Furthermore, in the North of the Netherlands, existing gas fields can be repurposed for hydrogen storage, while retrofitting existing national gas infrastructure to carry hydrogen and shifting the expertise in the oil and gas sector towards hydrogen production (Gigler et al. 2022, Interviewee 4, 26-04-23). This repurposing allows for cost-effective method utilization of green hydrogen in the Netherlands. However, as the market expands, predicting the exact future price of green hydrogen is challenging due to various factors. These include advancements in scale and production of electrolyzers technology, the cost of offshore renewable energy sources, and government policies and incentives (Interviewee 3, 12-04-23, Interviewee 6, 09-05-23). While current prices for green hydrogen may be relatively high, it is anticipated that economies of scale and technological advancements will lead to cost reductions in the future. Additionally, the establishment of cross-border collaborations in Europe can further contribute to price stabilization and competitiveness (Aurora Energy Research, 2022). Therefore, it is assumed that the price of the hydrogen will be 4 €/kg.

As current offshore wind projects continue to advance and mature, they are becoming increasingly cost-efficient to the point where subsidies are no longer necessary. The competitive nature of the offshore wind market has fostered innovation and encouraged renewable developers to optimize their operations to achieve higher cost-effectiveness (Interviewee 6, 09-05-23). As a result, the cost of generating electricity from offshore wind has significantly decreased, making it a financially attractive option without the need for government subsidies. Additionally, future wind farm tenders are expected to incorporate the integration of FPV and hydrogen technologies into their proposal. Combining wind farms with FPV systems and hydrogen systems allows developers to demonstrate a higher capacity rate. By including FPV and hydrogen integration in wind farm tenders, governments, and energy

stakeholders can promote sustainable and integrated approaches to energy generation, storage, and utilization, further advancing the energy transition.

G. Scenario Descriptions

Scenario 1: 700 MW HVAC

In the scenario, there are 47 wind turbines of 15 MW and 2500 solar panels of 400 Wp per 1 MWp. For every 100 MWp, there are 400 inverters of 250 kW to facilitate the conversion of DC power from solar panels to AC power for grid integration. The 66 kV HVAC cable inter-array cable length for the wind turbines spans approximately 70 kilometers, while for FPV systems, it covers 10.29 kilometers per 100 MWp. Additionally, there are two offshore and two onshore substations to control and distribute the generated energy. Lastly, the system utilizes four 220 kV AC export cables to transmit the electricity to the onshore grid. These factors have been doubled for the redundancy within the Dutch electrical grid in all scenarios.

Table 3: Overview of the number of each electrical components in the 700 MW HVAC Scenario

Number of Wind turbines	Number of Solar Panels per 1 MWp	Number of Inverters per 100 MWp	Length of Inter array Cables Wind (km)	Length of Inter array Cables FPV per 100 MWp (km)	Number of offshore & onshore substation	Number of 220 kV export cables
47	2500	400	70	10.29	4	4

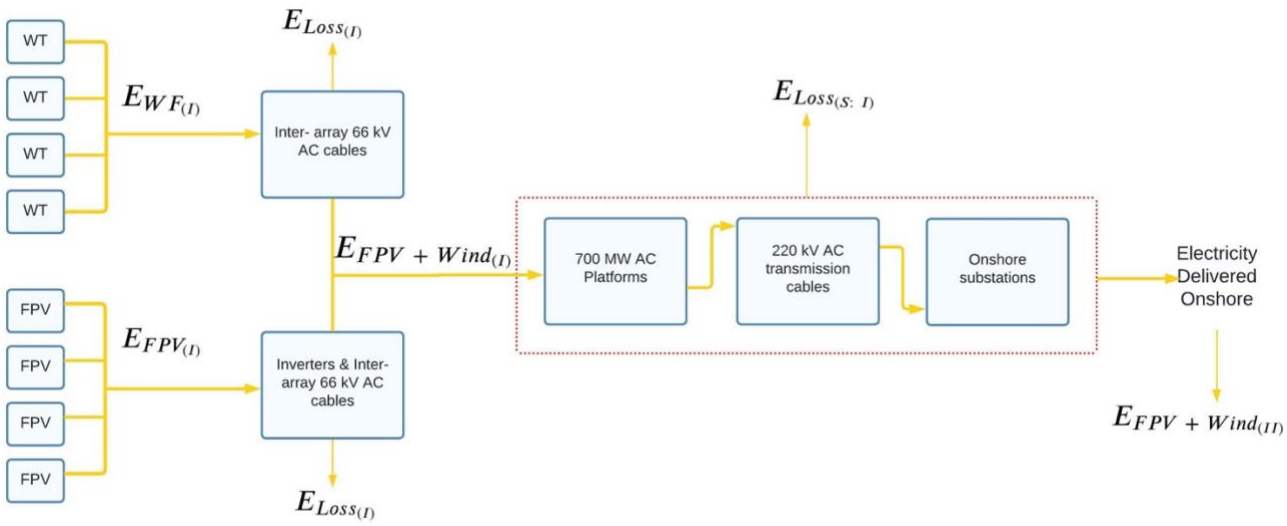

Figure 5: Overview of the components and relation to the methods and equations for 700 MW HVAC Scenario

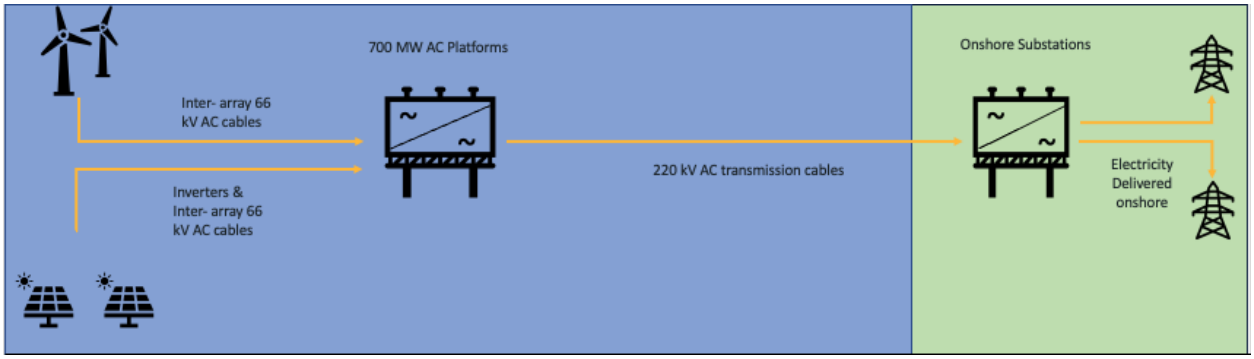

Figure 6: Overview of the component's location for 700 MW HVAC Scenario

Scenario 2: 2 GW HVDC VSC

In this scenario, the wind farm consists of 134 wind turbines of 15 MW, while similar to the previous scenario, for every 1 MWp there are approximately 2500 solar panels of 400 Wp installed, and 400 inverters of 250 kW employed per 100 MWp. The HVAC inter-array cable length for the wind turbines spans approximately 197 kilometers, ensuring connectivity and transmission within the wind farm. Additionally, for FPV systems, the inter-array cable length is approximately 10.29 kilometers per 100 MWp. The system is supported by two offshore AC/DC and two onshore DC/AC conversion stations,

which play a crucial role in managing and distributing the energy from the wind and FPV farms. Furthermore, four 525 kV export cables are used to transmit the electricity efficiently to the onshore grid.

Table 4: Overview of the number of each electrical components in the 2 GW HVDC-VSC Scenario

Number of Wind turbines	Number of Solar Panels per 1 MWp	Number of Inverters per 100 MWp	Length of Inter array Cables Wind (km)	Length of Inter array Cables FPV per 100 MWp (km)	Number of offshore & onshore conversion stations	Number of 525 kV export cables
134	2500	400	197	10.29	2	1

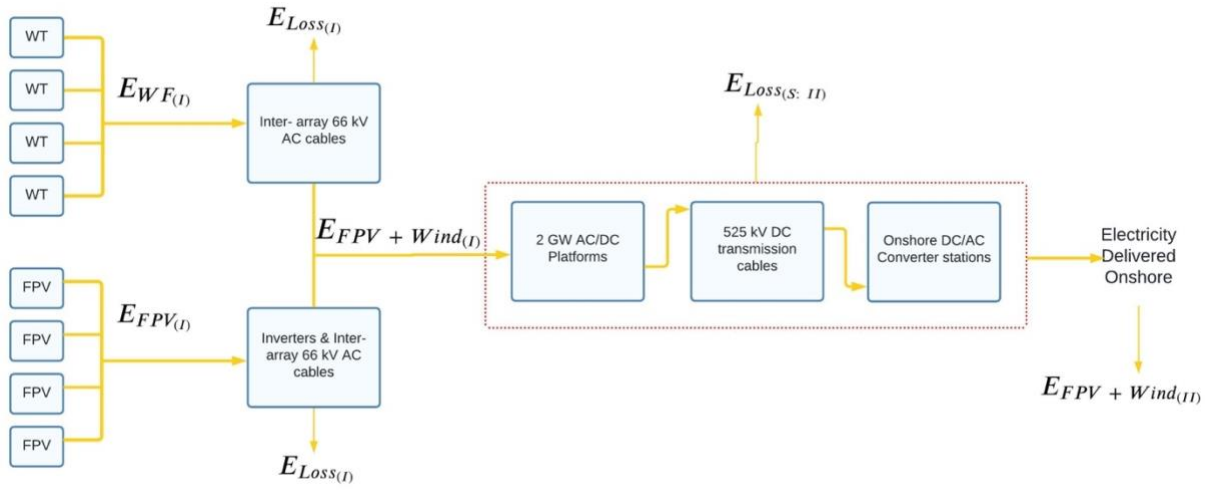

Figure 7: Overview of the components and relation to the methods and equations for 2 GW HVDC VSC Scenario

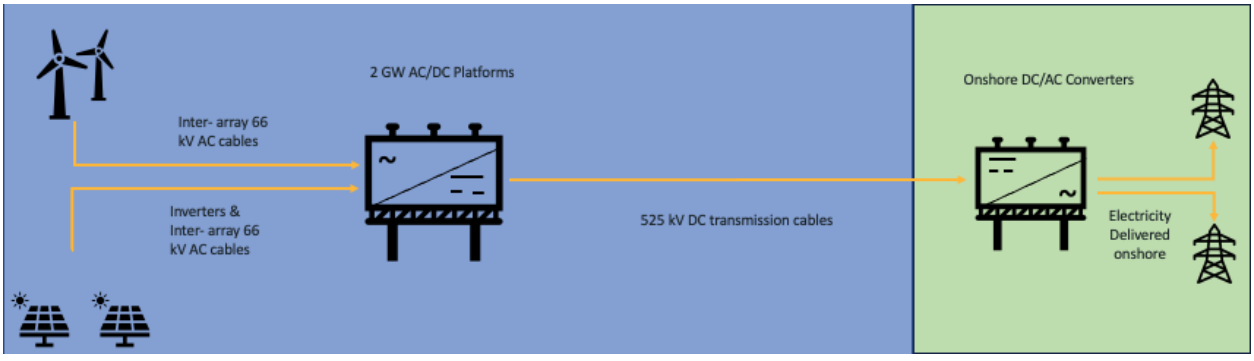

Figure 8: Overview of the component's location for 2 GW HVDC VSC Scenario

Scenario 3: 650 MW Hydrogen Production Plant & HPL

In this scenario, the wind farm consists of 47 wind turbines of 15 MW and incorporates various sizes of 100 MWp FPV installations. Additionally, the system includes a 650 MW offshore hydrogen production plant and a 120,000 nm^3/hr hydrogen pipeline. It assumed that all hydrogen that is delivered onshore is either has a direct demand connection, storage available, or converted back to electricity. Also, any wind and solar energy that is not utilized by the hydrogen production plant is curtailed.

Table 5: Overview of the number of each electrical and hydrogen components in the 650 MW Hydrogen production plant Scenario

Number of Wind turbines	Number of Solar Panels per 1 MWp	Number of Inverters per 100 MWp	Length of Inter array Cables Wind (km)	Length of Inter array Cables FPV per 100 MWp (km)	Number of Pipeline	Size of the pipeline
47	2500	400	70	10.29	1	400 mm

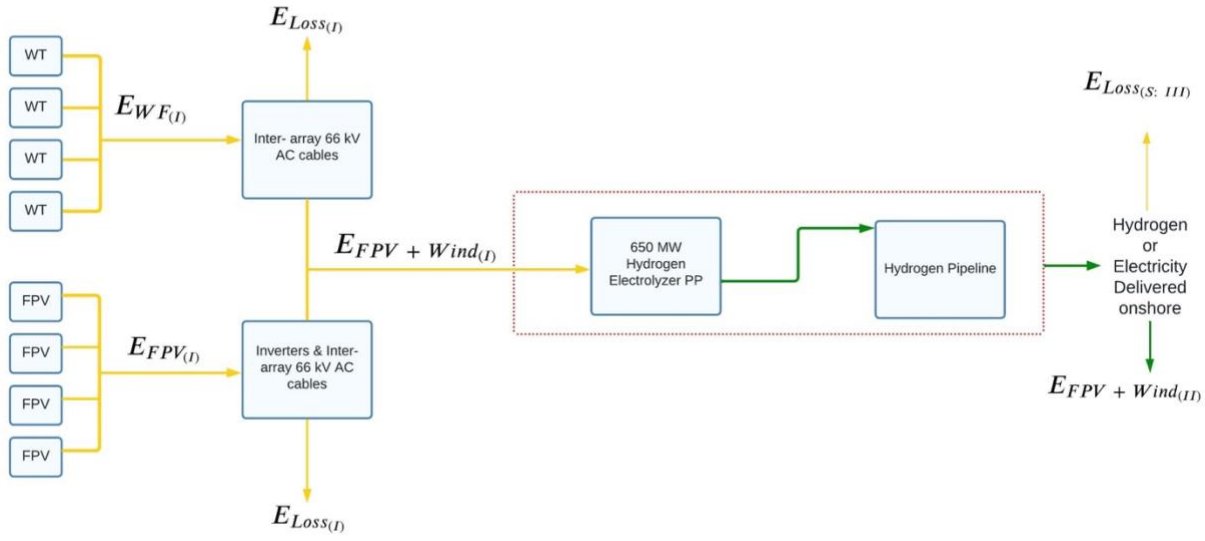

Figure 9: Overview of the components and relation to the methods and equations for 650 MW Hydrogen production plant & HPL Scenario

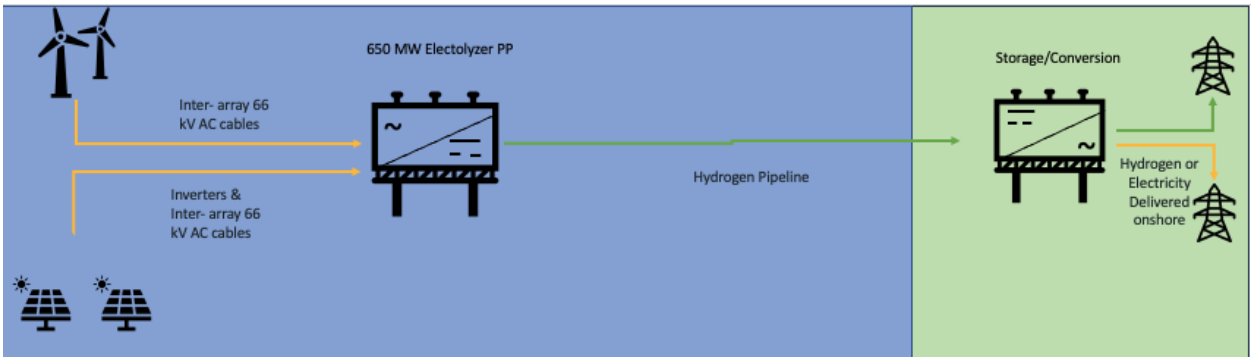

Figure 10: Overview of component's location for the 650 MW hydrogen PP

Scenario 4: 2 GW HVDC VSC + 650 MW Hydrogen Production Plant & HPL

In this scenario, the wind farm consists of 134 wind turbines of 15 MW and incorporates various sizes of 100 MWp FPV installations connected to 2 GW HVDC VSC system and the 650 MW offshore hydrogen production plant and a 120,000 nm^3/hr hydrogen pipeline. Given the priority, the energy will be directed towards that transmission method and any excess energy will be diverted to the other transmission method. This scenario contains all the same components and costs as Scenario 2 and 3.

Table 6: Overview of the number of each electrical and hydrogen components in the hybrid 2 GW HVDC and 650 MW Hydrogen production plant Scenarios with no energy transmission losses

Number of Wind turbines	Number of Solar Panels per 1 MWp	Number of Inverters per 100 MWp	Length of Inter array Cables Wind (km)	Length of Inter array Cables FPV per 100 MWp (km)	Number of offshore & onshore conversion stations	Number of 525 kV export cables	Number of Pipelines	Size of the pipeline
134	2500	400	197	10.29	2	1	1	400 mm

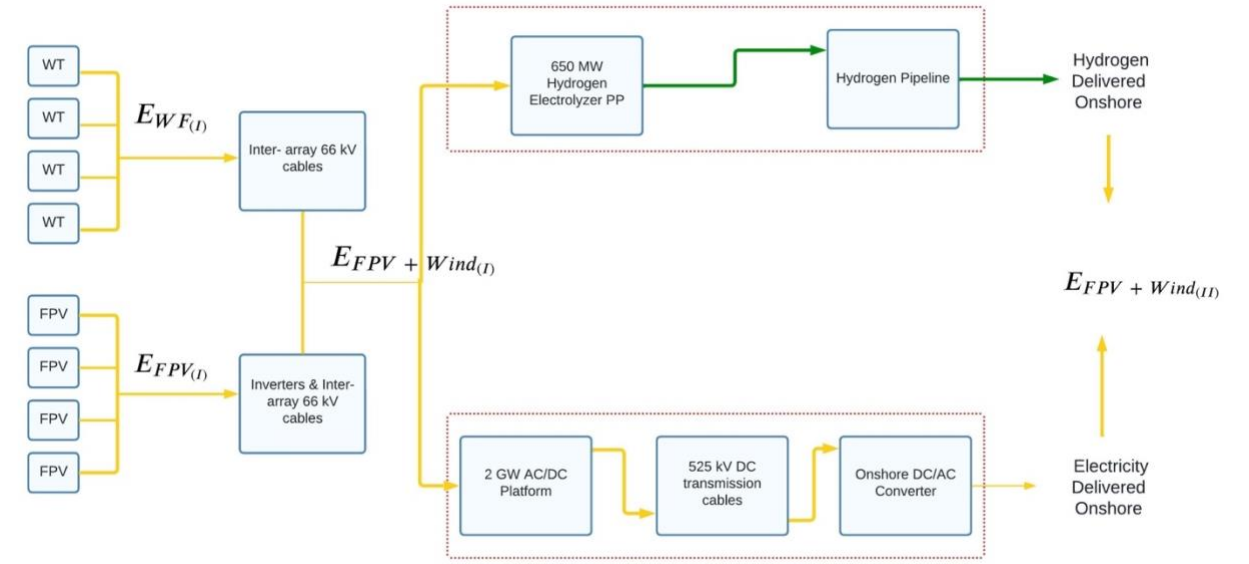

Figure 11: Overview of the components and relation to the methods and equations for the 2 GW HVDC VSC & 650 MW Hydrogen production plant & HPL Scenario with no energy transmission losses

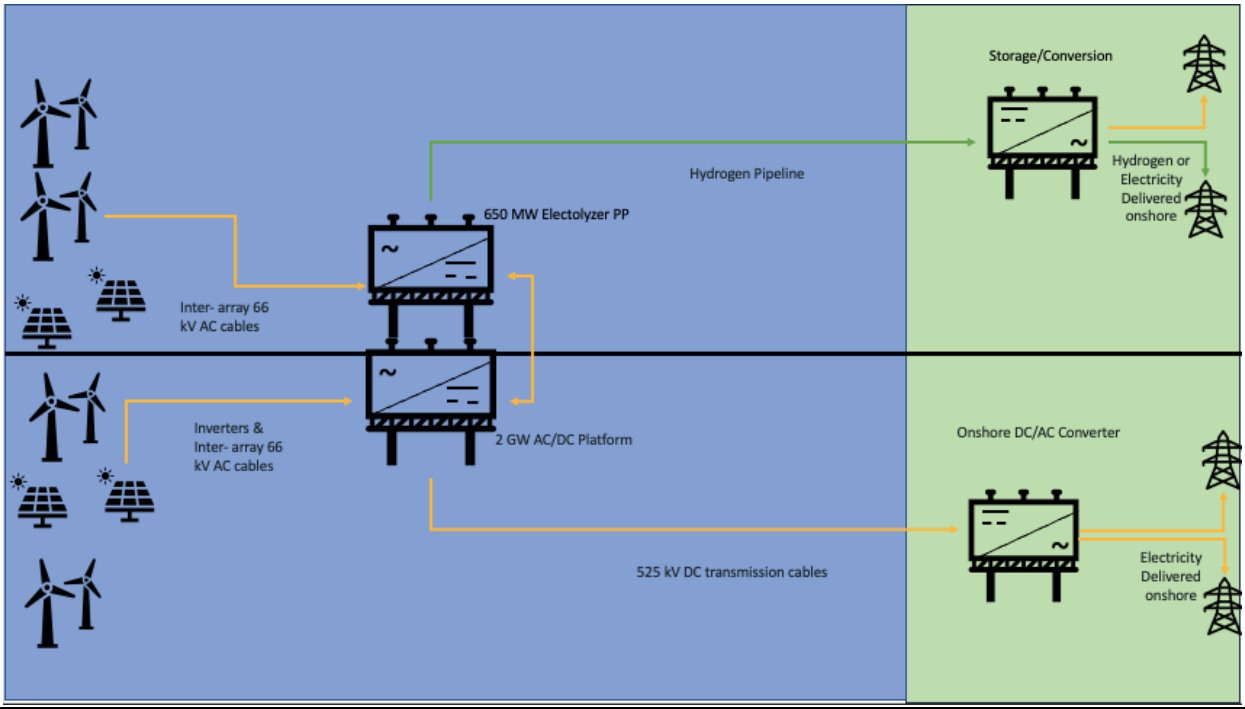

Figure 12: Overview of the component's location for 2 GW HVDC VSC & 650 MW Hydrogen production plant & HPL Scenario with no energy transmission losses

3. Results and Discussion

A. Results

Scenario I: 700 MW HVAC

Mean Energy Production

Figure 13, 14, and 15 illustrates the hourly mean energy generation of a wind farm with a capacity of 705 MW, along with a 300 MWp FPV farm, for the year 2013. The increased capacity of the FPV farm led to more efficient utilization of the cables, allowing for the transportation of greater amounts of energy during that year. The wind farm had a capacity factor of 65.34% and the FPV farm had a capacity factor of 11.31%, while the combined capacity factor with cable restrictions was 47.65% in 2013.

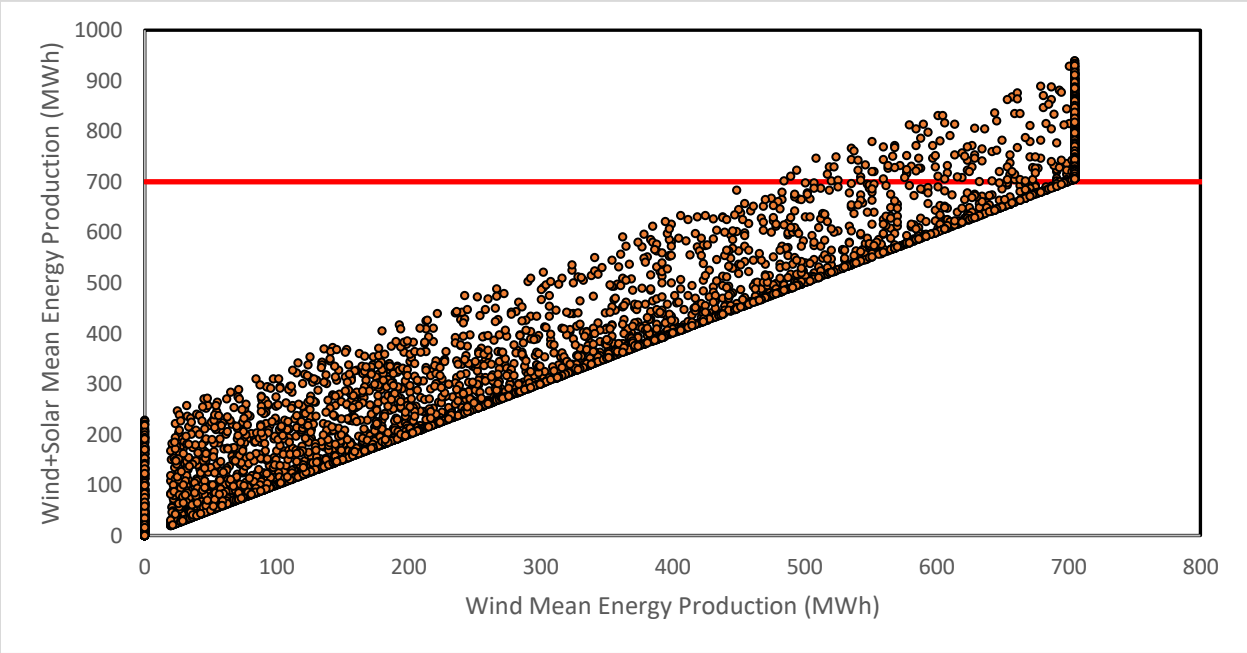

Figure 13: This scatterplot shows the correlation between only 705 MW wind farm mean energy production versus the total energy generation of the 705 MW wind farm and 300 MWp FPV farm with a red line at a maximum cable capacity of 700 MW.

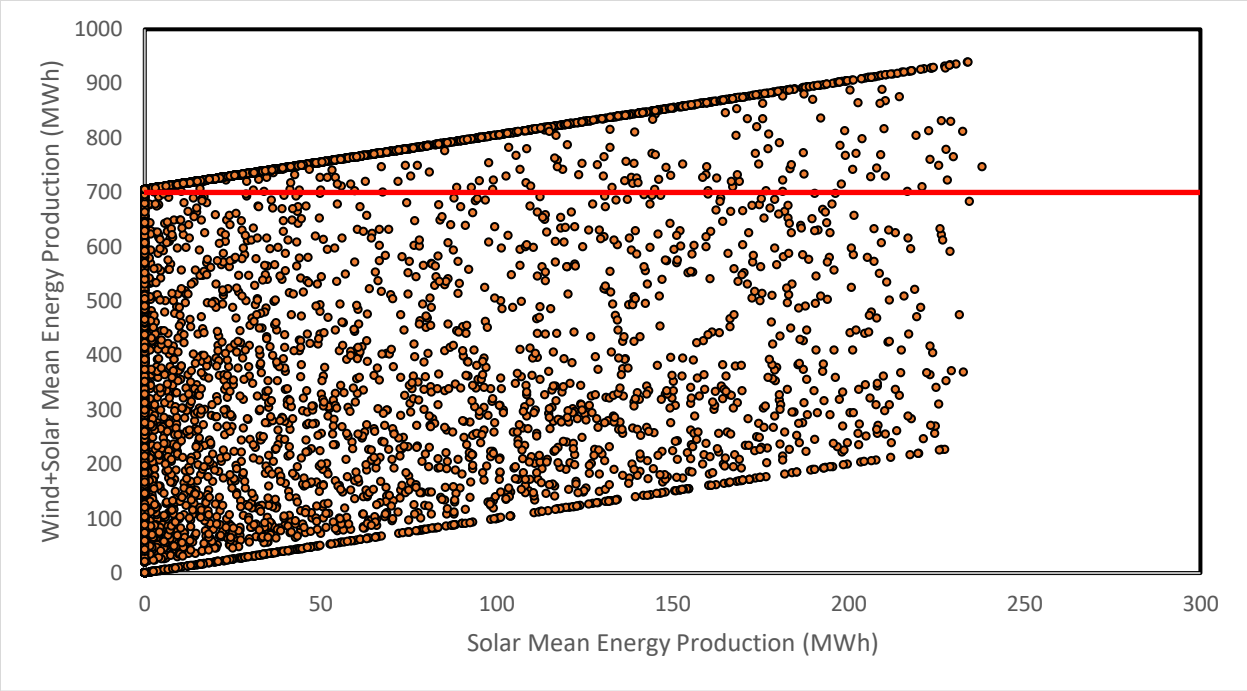

Figure 14: This scatterplot shows the correlation between only 300 MWp FPV farm mean energy production versus the total energy generation of the 705 MW wind farm and 300 MWp FPV farms with a red line at a maximum cable capacity of 700 MW.

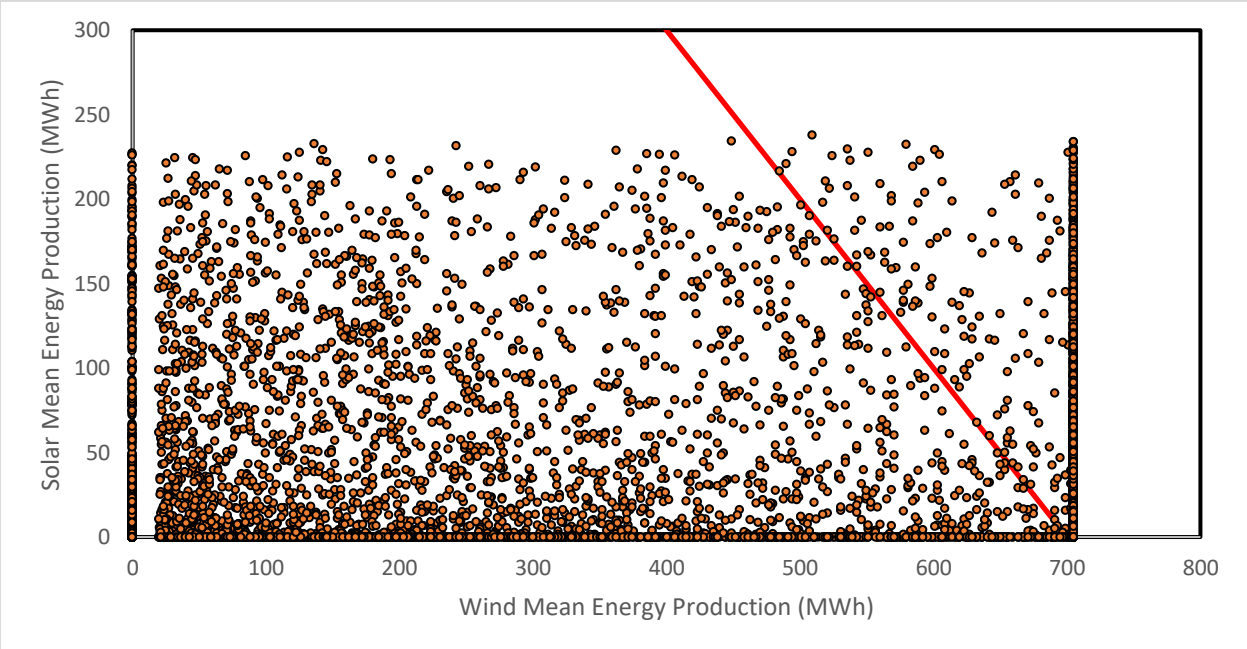

Figure 15: This scatterplot shows the correlation between only 300 MWp FPV farm mean energy production versus only the 705 MW wind farm mean energy production with a red line at a maximum cable capacity of 700 MW.

In the base year for a 300 MWp FPV system, there are 4,483 hours when $E_{FPV_{(h)}} > 0$, and out of these hours, there are 1,956 hours at maximum rated cables capacity when $E_{WT_{(h)}} > 700$ and 2,527 hours below rated cables capacity with the difference occurring during the 326 hours when $E_{FPV_{(h)}} > 0$ and $E_{WT_{(h)}} = 0$. Also, there were 4,157 hours where both the FPV farm, $E_{FPV_{(h)}} > 0$, and the wind farm, $E_{WT_{(h)}} > 0$, were operational. Out of these 4,157 hours, the combined wind and FPV farm operated at full capacity only 50% of the time, indicating that there was room for additional solar energy to be integrated. During these hours, there was no wind energy generation and only solar energy generation for 8% of the time, while for 42% of the time, the combined farms produced less than their rated energy generation. These results are linked to the power curve of the Vestas wind turbine. The wind farm operates at full capacity within a wind speed range of 9.88 - 31 m/s, while the less than rated capacity and only solar energy generation occur within the range of 3 - 31 m/s and 0 - 3 m/s, respectively. The wind farm's rated capacity is 705 MW, which is due to the wind turbines being slightly overplanted. This overplanting leads to more frequent instances where the cable capacity reaches its maximum and curtailment of wind and solar energy is necessary. In 2013, the curtailment of wind and solar energy generation amounted to 137 GWh, accounting for 3.2% of the total energy generation. The table highlights two key observations: adding FPV systems to the wind farm increase the number of hours where the cable reaches rated capacity and the corresponding increase in curtailed wind and solar energy.

Table 7 shows the impact of adding multiples of 100 MWp PV capacity to a 705 MW wind farm with a maximum cable capacity of 700 MW.

FPV Capacity (MWp)	Number of hours > 700 MWh for $E_{FPV_{(h)}} > 0$ & $E_{WT_{(h)}} > 0$	Total Energy Generation (GWh)	Mean Energy Generation (GWh)	Wind Curtailment (GWh)	Wind Curtailment (%)	FPV Curtailment (GWh)	FPV Curtailment (%)	Total curtailment (GWh)
0	0	4,035	4,014	21	0.52	0	0	21
100	1,993	4,134	4,076	49	1.18	9	0.22	58
200	2,036	4,233	4,137	74	1.76	22	0.52	96
300	2,098	4,332	4,161	96	2.21	41	0.96	137

Energy Transmission Losses

Figure 16 and 17 depicts the hourly energy transmission losses of a wind farm with a capacity of 705 MW, in conjunction with a 300 MWp FPV farm, for the year 2013. The wind farm had a capacity factor of 59.07% and the FPV farm had a capacity factor of 11.17%, with a combined capacity factor of 42.42% following energy loss before the platforms, denoted as $E_{Loss(I)}$. After accounting for the energy loss from the substation and export cables, denoted as $E_{Loss_{S:I}}$, the combined capacity factor was 41.06%. Due to the impact of the wake effect and transmission losses, the capacity factor experiences a reduction of 6%.

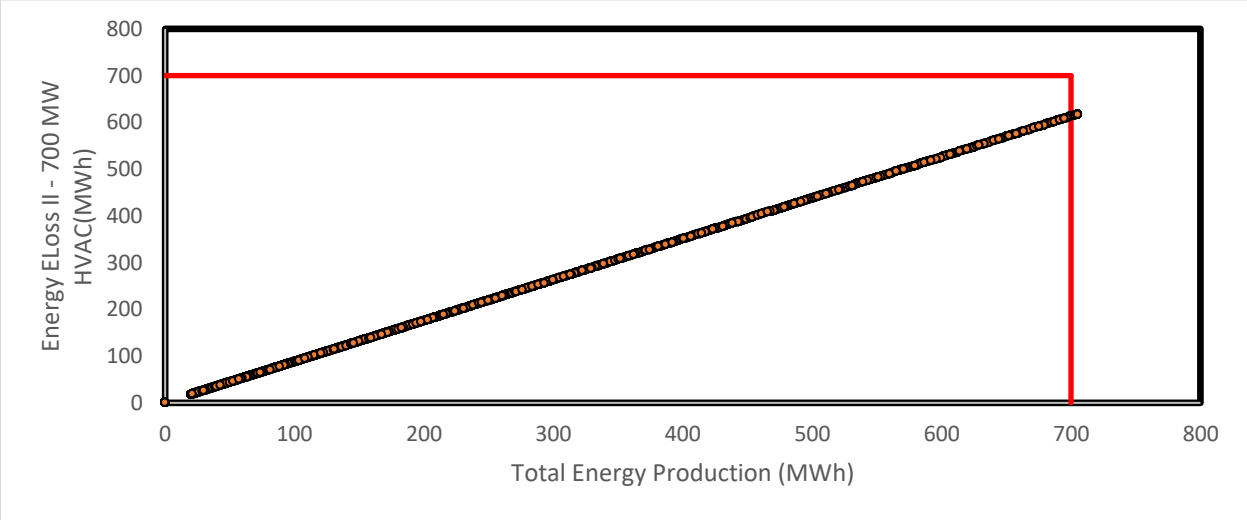

Figure 16: This scatterplot shows the correlation between only the 705 MW wind farm energy transmission losses versus the total energy generation of the 705 MW wind farm with a red line at a maximum cable capacity of 700 MW.

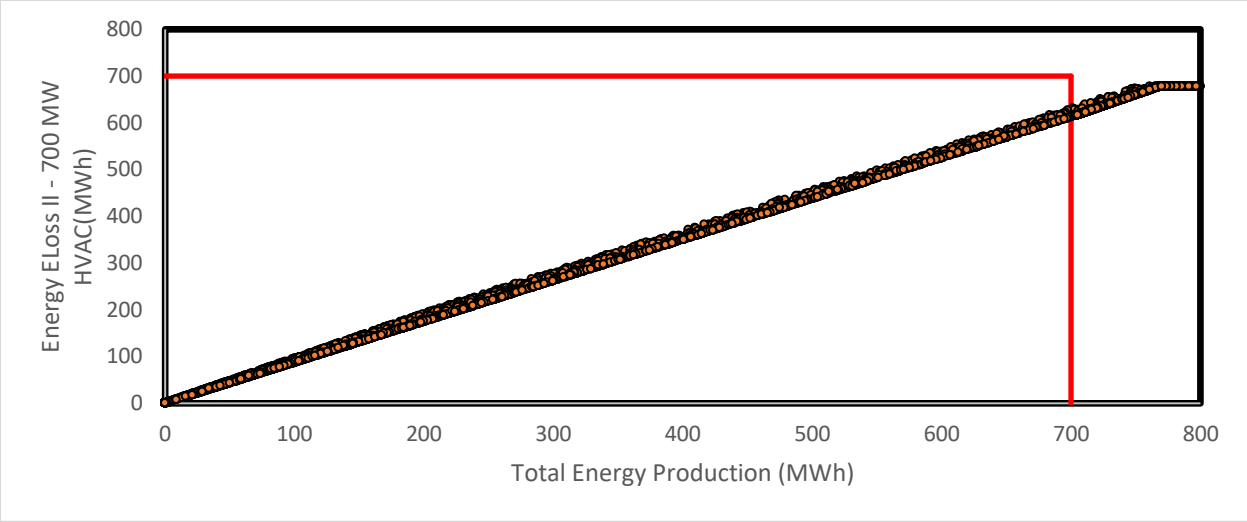

Figure 17: This scatterplot shows the correlation between 705 MW wind farm and 300 MWp FPV farm MW energy transmission losses versus the total energy generation of the 705 MW wind farm and 300 MWp FPV farm a red line at a maximum cable capacity of 700 MW.

In terms of operational hours, the combined operation of the FPV farm and wind farm remained the same. However, there were changes in the distribution of fully operational capacity and less than rated capacity. Due to the wake effect and transmission losses, the wind farm operates all 8,178 hours, when $E_{WT_{(h)}} > 0$, is below the rated capacity of the cable. As the wake effect and transmission losses drastically reduce the number of hours the cable reaches maximum capacity, the adding of FPV systems still increases the utilization of the cable by delivering more energy onshore. During the same operating 4,517 hours, there was no wind energy generation, and only solar energy was unvaried for 8% of the time. While the combined farms operated at full capacity for 16% of the time and operated at less than rated generation capacity for 76% of the time. In conclusion, when comparing the total energy generation of combined farms without cable capacity restrictions to the energy delivered onshore under cable restrictions and accounting for transmission losses, it becomes evident that incorporating an FPV system leads to an increase in the number of hours when the cable capacity is reached. Additionally, there is an associated increase in energy losses during transmission and curtailment of wind and solar energy. The impact of adding 100 MWp to the 705 MW wind farm is outlined in Table 8. The table highlights the same key finding as before that adding FPV systems increases the number of hours where the cable limit is exceeded, and the corresponding decrease in energy delivered onshore to total energy generation with increased curtailment and transmission losses.

Table 8 shows the impact of transmission losses of hybrid system from adding multiples of 100 MWp PV capacity to a 705 MW wind farm with a maximum cable capacity of 700 MW.

FPV Capacity (MWp)	Number of hours $E_{FPV_{(h)}} > 0$ & $E_{WT_{(h)}} > 0$	Number of hours > 700 MWh w/ $E_{Loss(I)}$	Number of hours 700 MWh > & > 0 MWh w/ $E_{Loss(I)}$	Number of hours wind = 0 MWh and solar > 0 MWh	Delivered Energy Onshore to National Grid (GWh)	Delivered Energy Onshore to National Grid/ Total Energy Generation (%)
0	0	0	8,178	0	3,531	87.51
100	4,157	57	3,774	326	3,625	87.70
200	4,157	438	3,393	326	3,706	87.55
300	4,157	684	3,147	326	3,776	87.17

Lifetime Production and Costs

Table 9 outlined the lifetime energy generation and capacity by adding 100 MWp to the 705 MW wind farm. The lifetime benefits from electricity sold and the LCOE are listed in table 10. The key takeaway from this analysis is that the integration of FPV systems leads to an increase in lifetime energy generation and associated benefits. However, it also results in a decrease in the lifetime capacity factor due to factors such as degradation, curtailment, and transmission losses. Finally, the LCOE could be much lower if transmission losses were not factored in.

Table 9 shows the impact of lifetime energy generation of hybrid system including transmission losses and degradation from adding multiples of 100 MWp PV capacity to a 705 MW wind farm with a maximum cable capacity of 700 MW.

FPV Capacity (MWp)	Lifetime Energy Generation (GWh)	Lifetime Capacity Factor [%]
0	66,744	54.04
100	67,580	47.92
200	68,726	43.35
300	69,818	39.65

Table 10 shows lifetime benefit and LCOE from adding multiples of 100 MWp PV capacity to a 705 MW wind farm with a maximum cable capacity of 700 MW.

FPV Capacity (MWp)	Lifetime Benefit (M€)	LCOE (€/kWh)
0	3,004.14	0.01769
100	3,048.75	0.01795
200	3,106.04	0.01812
300	3,160.07	0.01829

Scenario II: 2 GW HVDC

Mean Energy Production

Figure 18, 19, and 20 illustrates the hourly mean energy generation of a wind farm and the FPV farm in the year 2013. The wind farm has a capacity of 2010 MW, while the FPV farm has a capacity of 300 MWp. Incorporating FPV capacity can enhance the cable utilization efficiency, as previously mentioned. In 2013, the wind farm had a capacity factor of 65.34% and the FPV farm remained with a capacity factor of 11.31%, while the combined capacity factor with cable restrictions was 57.57%.

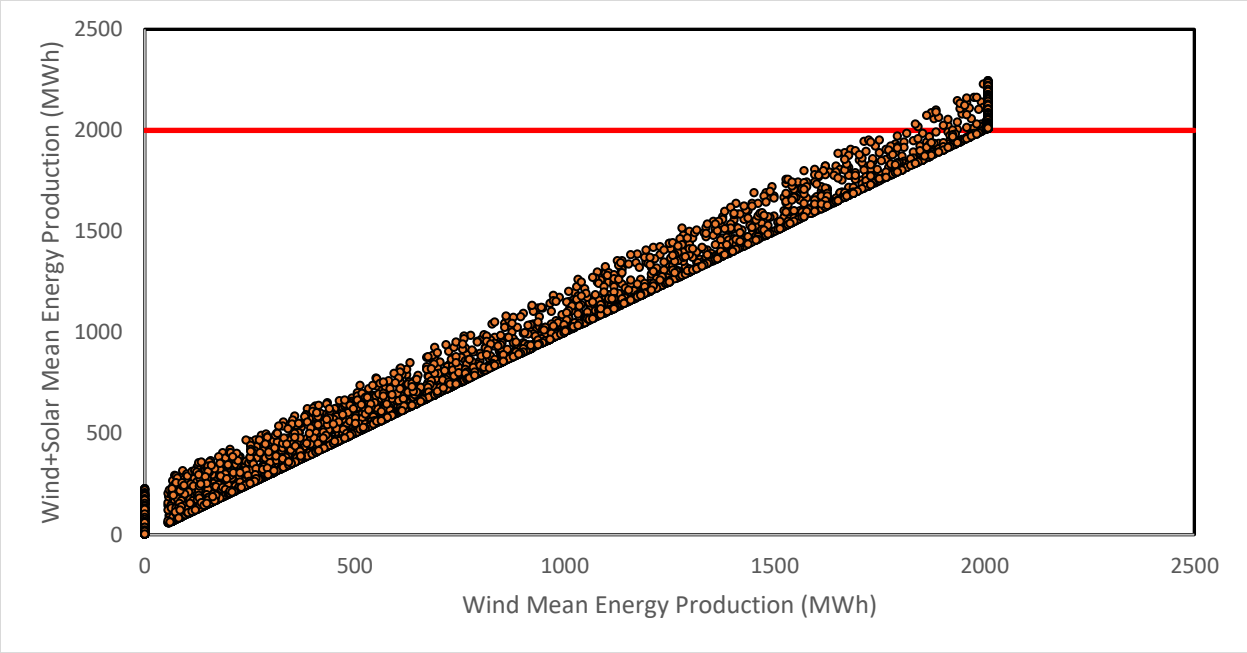

Figure 18: This scatterplot shows the correlation between only 2010 MW wind farm mean energy production versus the total energy generation of the 2010 MW wind farm and 300 MWp FPV farm with red line at maximum cable capacity of 2000 MW.

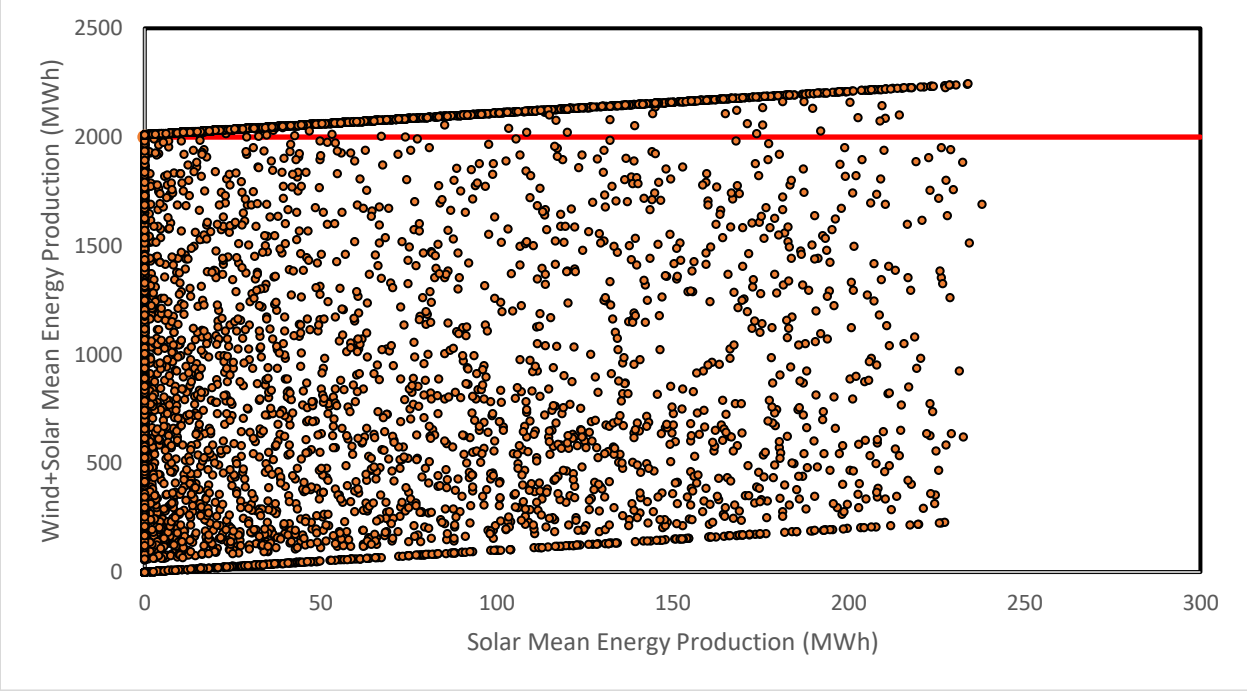

Figure 19: This scatterplot shows the correlation between only 300 MWp FPV farm mean energy production versus the total energy generation of the 2010 MW wind farm and 300 MWp FPV farms with red line at maximum cable capacity of 2000 MW.

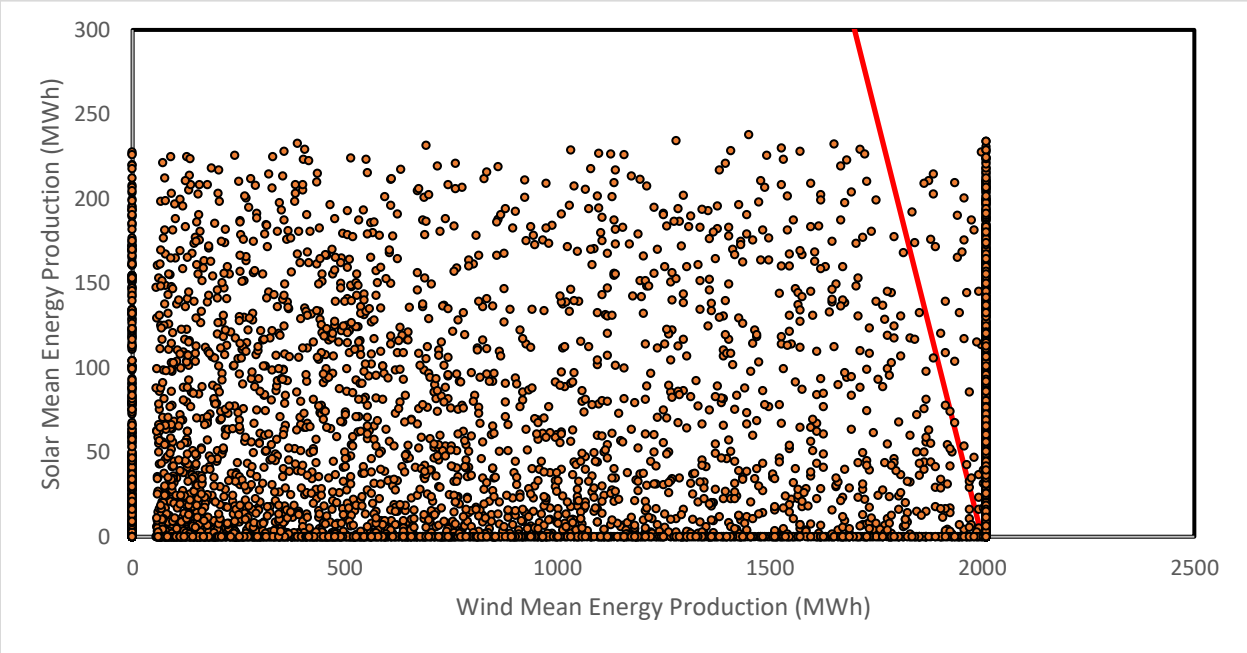

Figure 20: This scatterplot shows the correlation between only 300 MWp FPV farm mean energy production versus only the 2010 MW wind farm mean energy production with the red line at maximum cable capacity of 2000 MW.

In the base year 2013, there are 4483 hours when $E_{FPV_{(h)}} > 0$, and out of these hours, there are 1,954 hours at maximum rated cables capacity when $E_{WT_{(h)}} > 2$ GW and 2,529 hours below rated cables capacity. For the 4,157 hours, the combined wind and FPV farm operated at full capacity 48% of the time indicating that there was potential for additional solar energy integration. During these operational hours, there is still no wind energy generation and only solar energy generation for 8% of the time. Moreover, for 44% of the time, the combined farms produced less than their rated energy generation. This wind farm's rated capacity is 2010 MW, which is slightly overplanted also. In 2013, the curtailment of wind and solar energy generation amounted to 153 GWh, accounting for 1.3% of the total energy generation. Like scenario 1, incorporating FPV systems into a 2010 MW farm, this enhances the utilization of cables and allows for increased energy delivery onshore. Nevertheless, this intensifies the curtailment of the wind and FPV farms as the cable capacity is more frequently reached. The impact of adding 100 MWp to the 705 MW wind farm, including the associated changes in curtailment, is presented in Table 11. Also, this table highlights the same two key observations from Scenario 1: the increase in the number of hours where the cable limit is exceeded and the corresponding increase in curtailed wind and solar energy.

Table 11 shows the impact of adding multiples of 100 MWp PV capacity to a 2010 MW wind farm with a maximum cable capacity of 2000 MW.

FPV Capacity (MWp)	Number of hours > 2000 MWh for $E_{FPV_{(h)}} > 0$ &/or $E_{WT_{(h)}} > 0$	Total Energy Generation (GWh)	Mean Energy Generation (GWh)	Wind Curtailment (GWh)	Wind Curtailment (%)	FPV Curtailment (GWh)	FPV Curtailment (%)	Total curtailment (GWh)
0	4,156	11,505	11,463	42	0.37	0	0.0	42
100	1,968	11,604	11,526	69	0.59	9	0.08	78
200	1,981	11,703	11,588	97	0.83	18	0.16	115
300	1,991	11,802	11,650	127	1.07	26	0.22	153
400	2,002	11,901	11,710	155	1.30	36	0.30	191
500	2,021	12,000	11,771	172	1.43	57	0.48	229

Energy Transmission Losses

Figure 21 and 22 depicts the hourly energy transmission losses of a wind farm with a capacity of 2010 MW, in conjunction with a 300 MWp FPV farm, for the year 2013. The wind farm had a capacity factor of 57.34% and the FPV farm had a capacity factor of 11.17%, with a combined capacity factor of 51.35% after considering the energy loss prior to the hydrogen production plant, $E_{Loss(I)}$. After factoring in the energy loss from the converter station and export cable, $E_{Loss_{S:I}}$, the combined capacity factor was 49.00%. As a result of the influence of the wake effect and transmission losses, there is a decrease of 8% in the capacity factor.

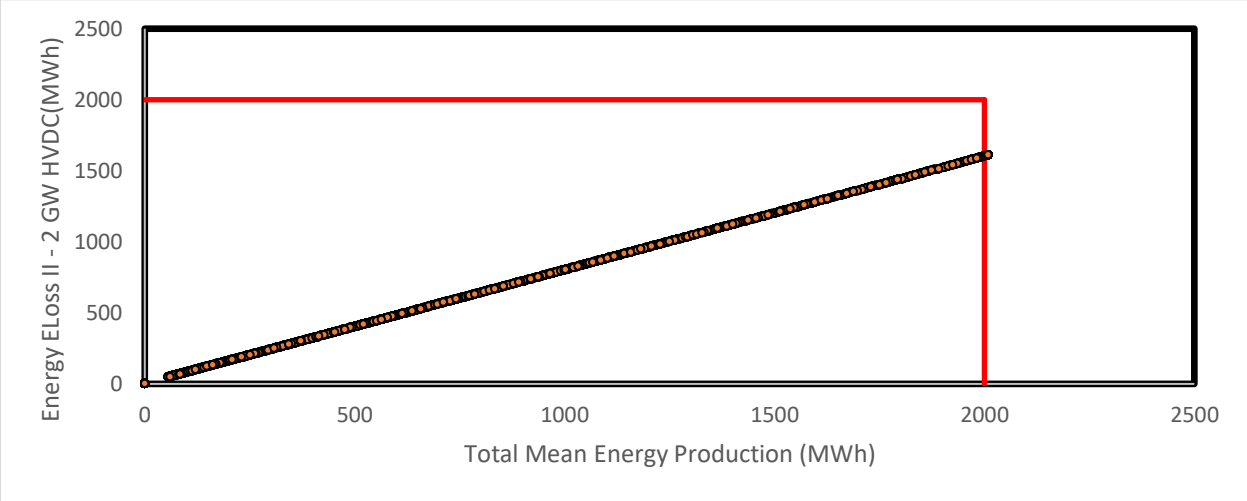

Figure 21: This scatterplot shows the correlation between only the 2010 MW wind farm energy transmission losses versus the total energy generation of the 2010 MW wind farm with red line at maximum cable capacity of 2000 MW.

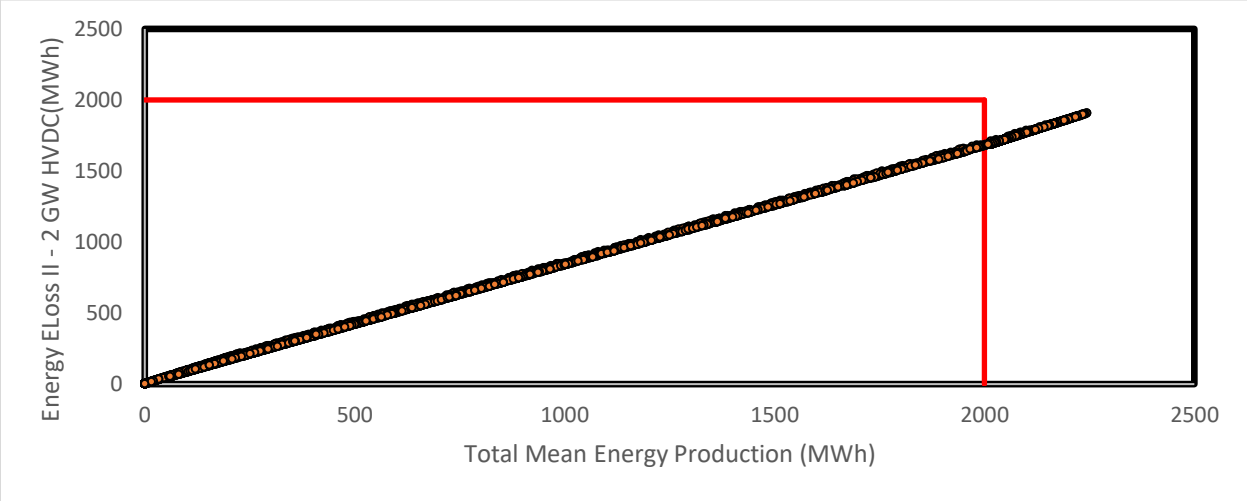

Figure 22: This scatterplot shows the correlation between 2010 MW wind farm and 300 MWp FPV farm MW energy transmission losses versus the total energy generation of the 2010 MW wind farm and 300 MWp FPV farm with red line at maximum cable capacity of 2000 MW.

In terms of operational hours, the combined operation of the FPV farm and wind farm remained the same. However, there were changes in the distribution of fully operational capacity and less than rated capacity. Due to the wake effect and transmission losses, the wind farm operates all 8,178 hours, when $E_{WT_{(h)}} > 0$, is below the rated capacity of the cable. With wake effect and transmission losses being more prominent in the 2 GW scenario, this results in the 4,157 operating hours to operate at full capacity for 0% of the time and operating at less than rated generation capacity for 100% of the time for the combined farms with still no wind energy generation and only solar energy generation for 8% of the time. The curtailment of wind and solar energy from maximum rated cable capacity only occurs in FPV larger than 400 MWp. In conclusion, while the incorporation of FPV systems leads to an increase in the amount of energy delivered onshore, more energy is lost through larger wake effects and transmission losses compared to scenario 1 and the total energy generation in this scenario. This highlights the significance of carefully considering the wake effect when designing and planning large-scale wind farms to optimize energy production and mitigate losses.

Table 12 shows the impact of transmission losses of hybrid system from adding multiples of 100 MWp PV capacity to a 2010 MW wind farm with a maximum cable capacity of 2000 MW.

FPV Capacity (MWp)	Number of hours $E_{FPV_{(h)}} > 0$ & $E_{WT_{(h)}} > 0$	Number of hours > 2000 MWh w/ $E_{Loss(I)}$	Number of hours 2000 MWh > & > 0 MWh w/ $E_{Loss(I)}$	Number of hours wind = 0 MWh and solar > 0 MWh	Delivered Energy Onshore to National Grid (GWh)	Delivered Energy Onshore to National Grid/ Total Energy Generation (%)
0	0	0	8,178	0	9,197	79.93
100	4,157	0	3,831	326	9,729	83.84
200	4,157	0	3,831	326	9,823	83.93
300	4,157	0	3,831	326	9,916	84.02
400	4,157	82	3,749	326	10,007	84.09
500	4,157	326	3,617	326	10,092	84.10

Lifetime Production and Costs

In Table 13, the lifetime energy generation and the benefits obtained from selling electricity are outlined, considering the addition of 100 MWp to the existing 2010 MW wind farm. Additionally, Table 14 provides the lifetime benefits and LCOE considering the degradation of wind and solar.

Comparing Scenario 1 to the conclusions of this scenario, the lifetime capacity is similar. However, there is a significant improvement in the lifetime benefit and generation, almost tripling compared to Scenario 1. Additionally, the high lifetime energy generation causes the LCOE to be lower as the rated capacity of the cable and the generation larger size of the wind and FPV farm result in a greater amount of energy being brought onshore. This indicates that despite the higher costs, the overall energy production and transmission capabilities of the wind and FPV farm are more substantial, leading to a greater supply of renewable energy to the onshore grid throughout its operational lifespan. Lastly, if we excluded the transmission losses from the LCOE calculations, there could be a slightly lower LCOE in this scenario.

Table 13 shows the impact of lifetime energy generation of hybrid system including transmission losses and degradation from adding multiples of 100 MWp PV capacity to a 2010 MW wind farm with a maximum cable capacity of 2000 MW.

FPV Capacity (MWp)	Lifetime Energy Generation (GWh)	Lifetime Capacity Factor (%)
0	184,734	52.53
100	185,270	50.12
200	186,463	48.16
300	187,650	46.37
400	188,826	44.72
500	189,964	43.20

Table 14 shows the lifetime benefits and LCOE from adding multiples of 100 MWp PV capacity to a 2010 MW wind farm with a maximum cable capacity of 2000 MW.

FPV Capacity (MWp)	Lifetime Benefit (M€)	LCOE (€/kWh)
0	8,314.87	0.01208
100	8,346.02	0.01218
200	8,406.75	0.01227
300	8,467.15	0.01237
400	8,526.83	0.01246
500	8,584.18	0.01255

Scenario III: 650 MW Hydrogen Electrolyzer Production Plant & HPL

Mean Energy Production

Figure 23, 24, and 25 depicts the average hourly energy generation for hydrogen derived from the combined energy generation of a wind farm, FPV farm, and hydrogen production plant in the year 2013. The hydrogen production plant, with a rated capacity of 650 MW, was interconnected with a 705 MW wind farm as well as several FPV farms of varying sizes. The capacity for the 650 MW hydrogen production plant in the wind only is 58.78%, while the 300 MWp and 500 MWp have a capacity factor of 61.92% and 63.63%.

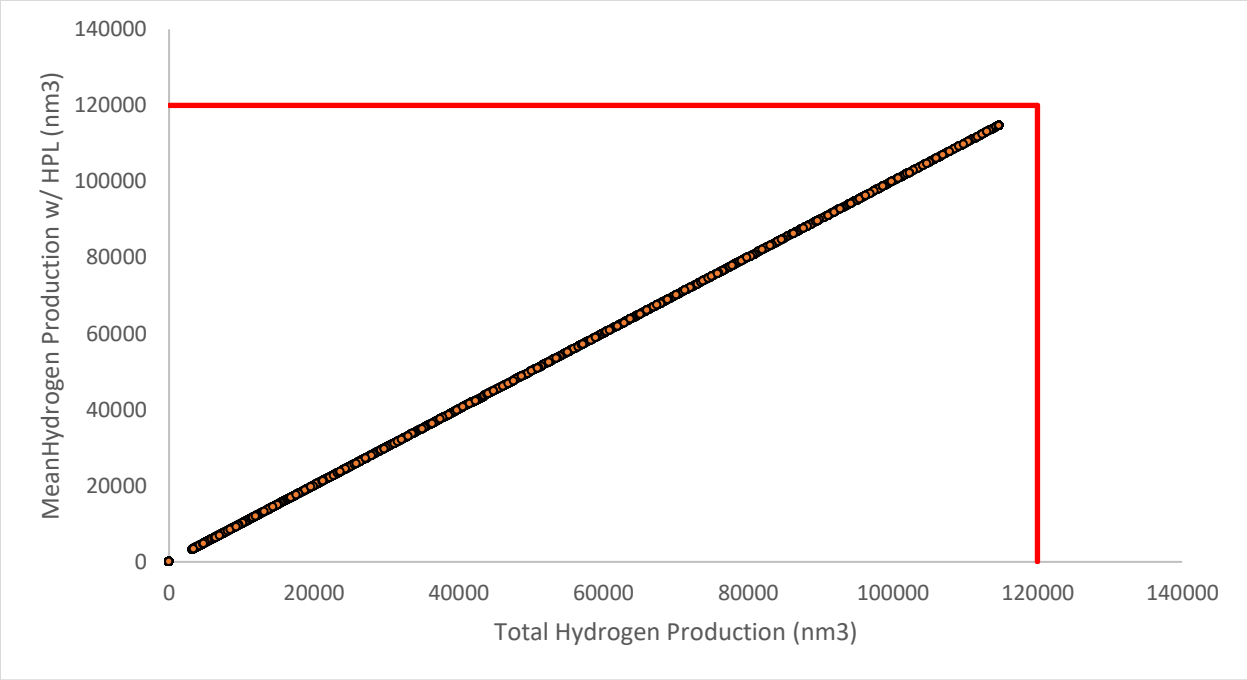

Figure 23: This scatterplot shows the correlation between only the 705 MW wind farm mean hydrogen production with HPL restrictions versus the total hydrogen generation of the 705 MW wind farm without HPL restrictions with red line at maximum flow rate capacity of 120,000 nm3.

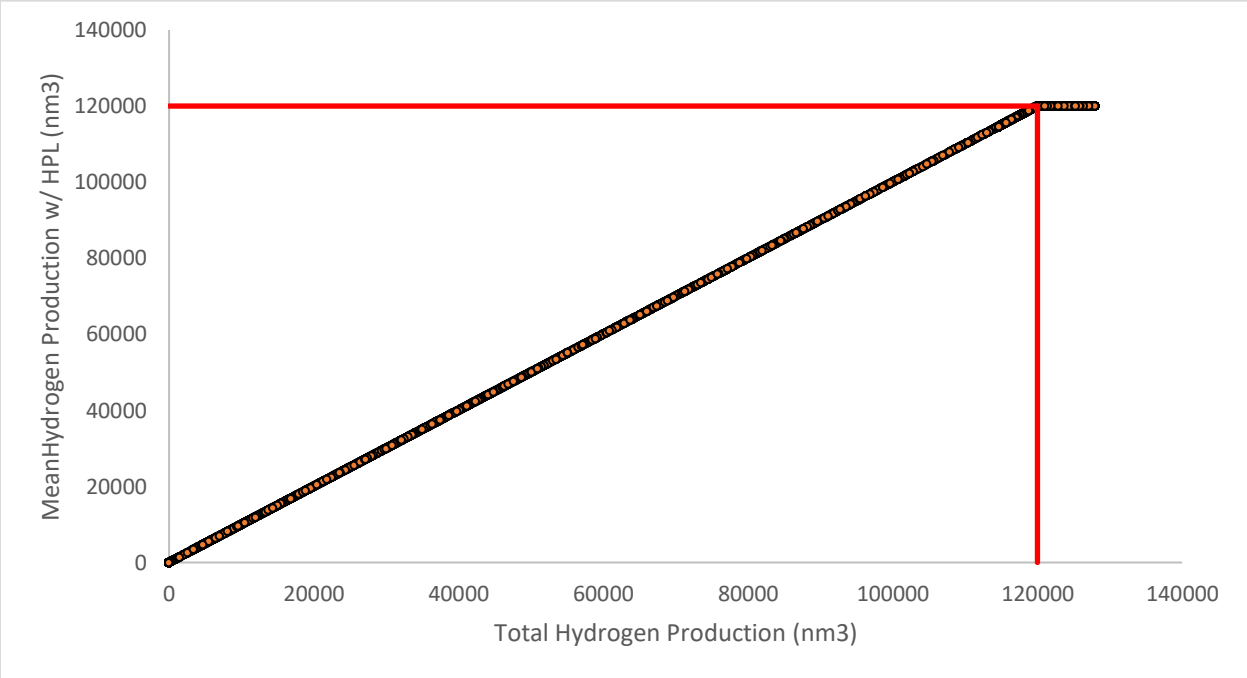

Figure 24: This scatterplot shows the correlation between 705 MW wind and 300 MWp farm mean hydrogen production with HPL restrictions versus the total hydrogen generation of the 705 MW wind and 300 MWp farm without HPL restrictions with red line at maximum flow rate capacity of 120,000 nm3.

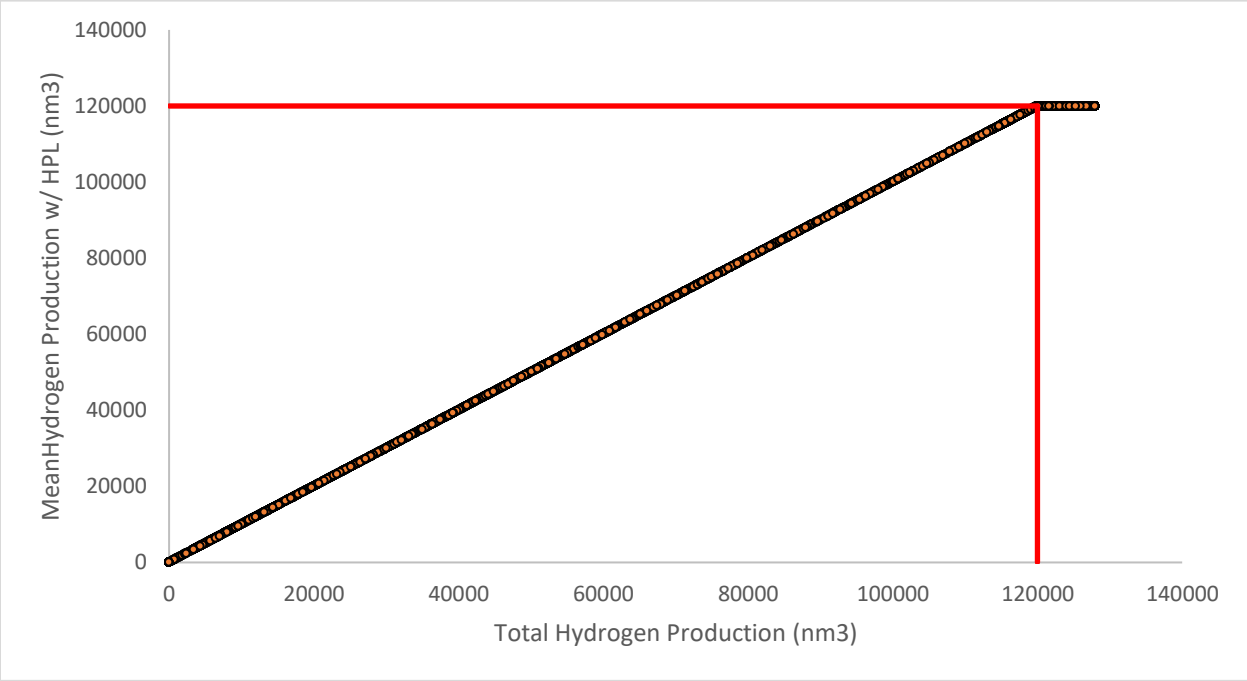

Figure 25: This scatterplot shows the correlation between 705 MW wind and 500 MWp FPV farm mean hydrogen production with HPL restrictions versus the total hydrogen generation of the 705 MW wind and 500 MWp farm without HPL restrictions with red line at maximum flow rate capacity of 120,000 nm3.

During the base year of 2013, when considering a 300 MWp FPV farm, it was observed that there were 8,178 operational hours in which $E_{H_{(h)}} > 0$. However, as the hydrogen production plant operates at a maximum net production rate with a requirement of 787 MWh, curtailment occurs during the hours when the wind and FPV farm generate energy above this threshold. This curtailment amounts to an annual total of 30 GWh. Furthermore, due to the limitations imposed by the maximum flow rate of the hydrogen pipeline, additional curtailment occurs at the hydrogen production plant to meet the pipeline restrictions. Among these hours, the hydrogen plant operated at the maximum flow rate for 1,093 hours, which accounts for approximately 13% of the total operating time. For the remaining 87% of the time, the hydrogen plant operated below the rated flow rate capacity of the pipeline. The hours during which the hydrogen plant operates above the maximum flow rate, resulting in curtailment, amount to an additional 38 GWh of energy loss. Comparing this scenario to the 300 MWp scenario in Scenario 1, it is evident that there is less curtailment. However, when considering the electricity available onshore based on the LHV of hydrogen, it becomes apparent that more than half of the energy is lost due to the conversion of electricity to hydrogen and back to electricity. This highlights the efficiency challenges associated with the conversion process for hydrogen.

Table 15 shows the impact of adding multiples of 100 MWp PV capacity to a 705 MW wind farm and a 650 MW Hydrogen production plant with a maximum pipeline capacity of 120000 nm^3

FPV Capacity (MWp)	Curtailment of Wind and Solar (GWh)	Number of hours > 120,000 nm^3	Number of hours 120000 nm^3 > & > 0 nm^3	Delivered Hydrogen Onshore (nm^3)	Delivered Hydrogen Onshore (kg)	Delivered Hydrogen Onshore/ Total Hydrogen Generation (%)	Hydrogen Converted to electricity w/ LHV (GWh)
0	0	0	8,178	656,334,818	58,696,610	100	1,969
100	7	409	8,095	671,335,303	60,038,117	99.83	2,014
200	25	808	7,696	683,157,604	61,095,396	99.41	2,049
300	37	1,093	7,411	693,839,589	62,935,443	99.14	2,082
400	47	1,306	7,198	703,732,679	63,762,042	98.91	2,111
500	56	1,477	7,027	712,975,560	63,762,042	98.73	2,139

Hydrogen Energy Transmission Losses

Figure 26, 27, and 28 illustrates the average hourly energy transmission losses for hydrogen production when combining a wind farm, FPV farm, and hydrogen production plant in the year 2013. The wind farm scenario operates the 650 MW hydrogen production plant at a capacity factor of 52.95%, while the 300 MWp and 500 MWp FPV farms has a capacity factor of 56.63% and 58.97%.

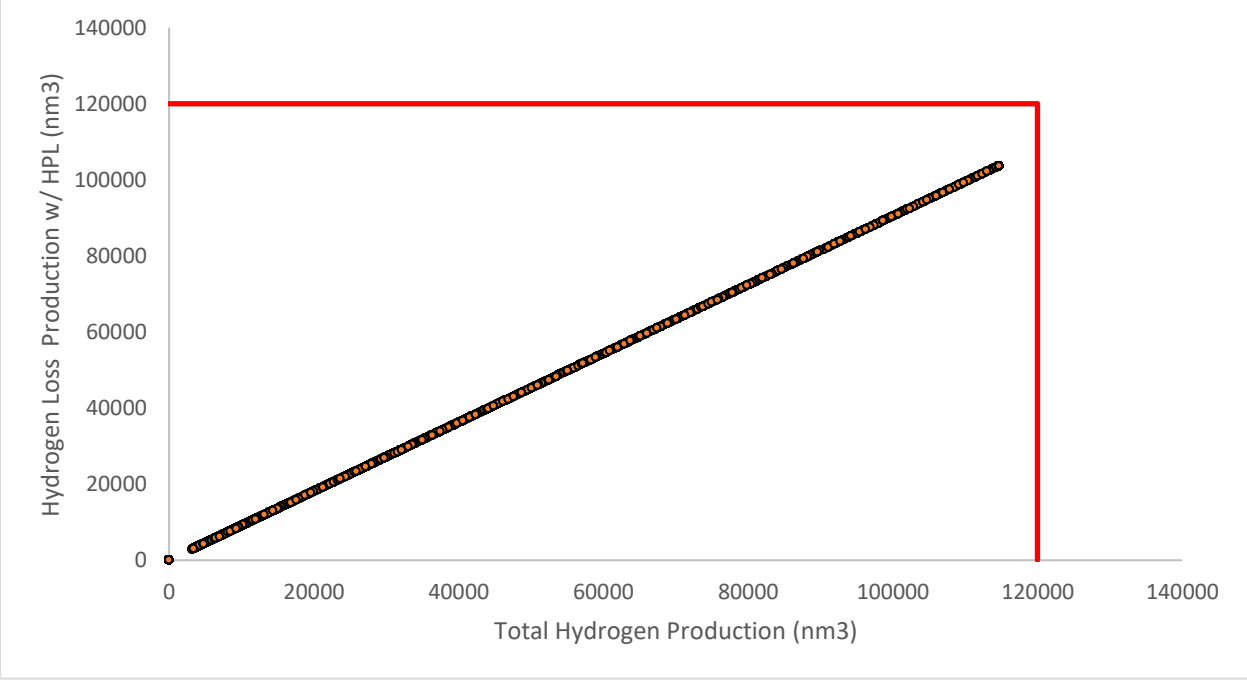

Figure 26: This scatterplot shows the correlation between 705 MW wind and 300 MWp farm energy transmission losses for hydrogen production with HPL restrictions versus the total hydrogen generation of the 705 MW wind and 500 MWp farm without HPL restrictions with red line at maximum flow rate capacity of 120,000 nm3.

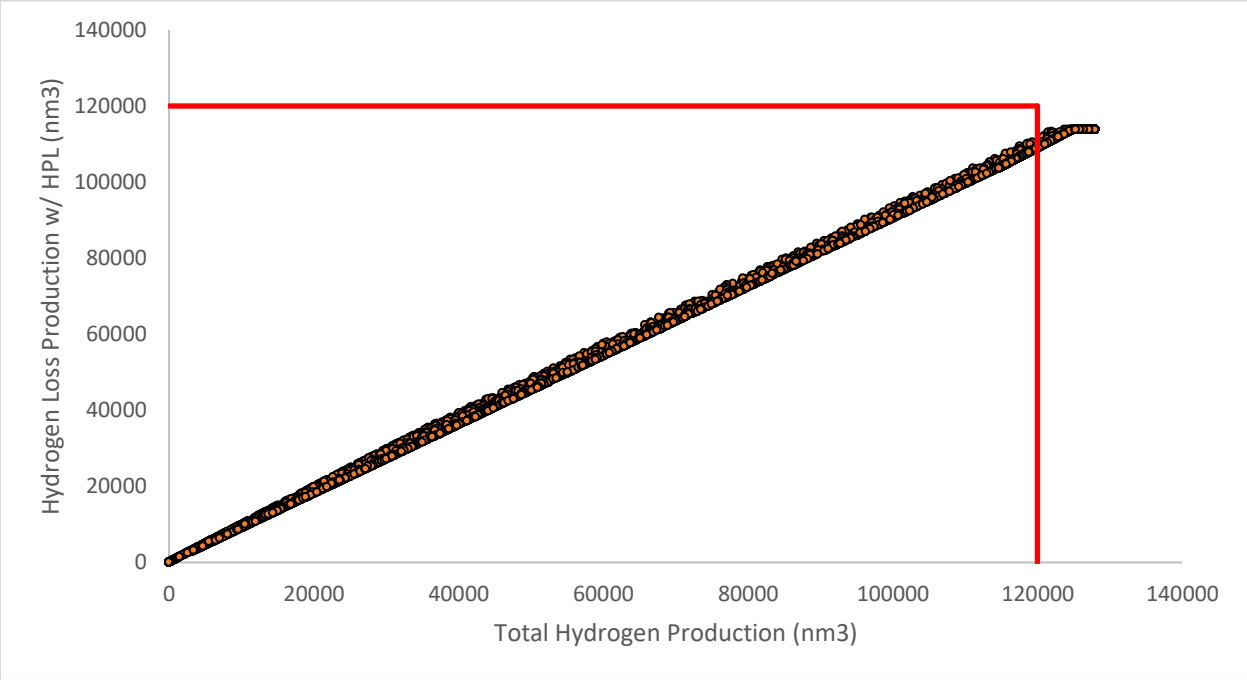

Figure 27: This scatterplot shows the correlation between 705 MW wind and 300 MWp farm energy transmission losses for hydrogen production with HPL restrictions versus the total hydrogen generation of the 705 MW wind and 500 MWp farm without HPL restrictions with red line at maximum flow rate capacity of 120,000 nm3.

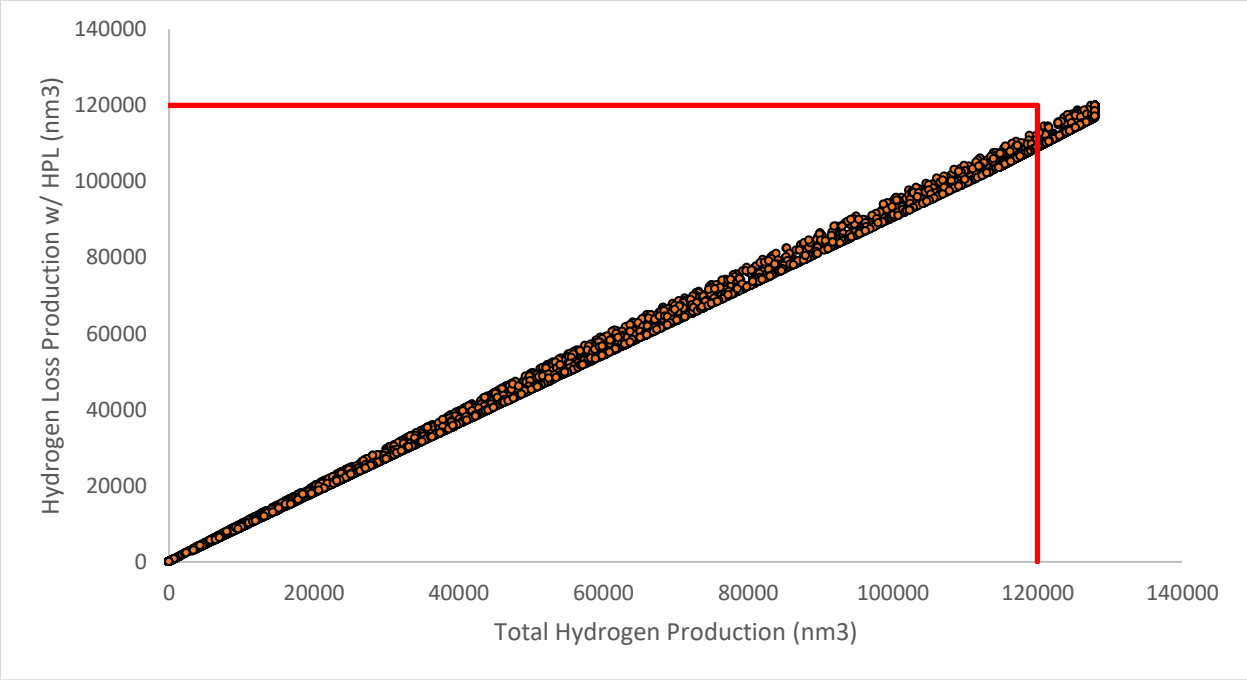

Figure 28: This scatterplot shows the correlation between 705 MW wind and 500 MWp farm energy transmission losses for hydrogen production with HPL restrictions versus the total hydrogen generation of the 705 MW wind and 500 MWp farm without HPL restrictions with red line at maximum flow rate capacity of 120,000 nm3.

During the base year of 2013, curtailment of wind and solar occurs only in the 400 MWp and 500 MWp layouts when the maximum net production rate of the hydrogen production plant is reached. This is mainly attributed to the wake effect and transmission losses from the wind and FPV farm. In the 400 MWp FPV farm, wind and solar energy curtailment amounts to a total of 21 GWh annually, increasing to 43 GWh in the 500 MWp farm. Furthermore, curtailment of hydrogen production resulting from pipeline restrictions is observed in the 400 MWp and 500 MWp scenarios. In the case of the 500 MWp FPV, the hydrogen plant operates at the maximum flow rate for 773 hours, accounting for approximately 9% of the total operating time. For the remaining 7,731 hours (about 91% of the time), the hydrogen plant operates below the rated flow rate capacity of the pipeline. The curtailment energy losses due to reaching the maximum flow rate capacity amount to 29 GWh in the 400 MWp scenario and 38 GWh in the 500 MWp scenario.

Similar to the mean energy production, when considering the electricity available onshore based on the LHV of hydrogen, it becomes evident that approximately half of the energy is lost during the conversion from electricity to hydrogen and back to electricity.

Table 16 shows the impact of transmission losses from adding multiples of 100 MWp PV capacity to a 705 MW wind farm and a 650 MW Hydrogen production plant with a maximum pipeline capacity of 120000 nm^3.

FPV Capacity (MWp)	Curtailment of Wind and Solar (GWh)	Number of hours $E_{H_{(h)}}$	Number of hours > 120,000 nm^3	Number of hours 120000 nm^3 > & > 0 nm^3	Delivered Hydrogen Onshore (nm^3)	Delivered Hydrogen Onshore (kg)	Delivered Hydrogen Onshore/ Total Hydrogen Generation (%)	Hydrogen Converted to electricity w/ LHV (GWh)
0	0	8,178	0	8,178	593290679	53,058,516	90.39	1,780
100	0	8,504	0	8,504	609,153,607	54,477,152	90.59	1,837
200	0	8,504	0	8,504	622,728,498	55,691,167	90.62	1,868
300	0	8,504	0	8,504	634,533,803	56,746,926	90.66	1,904
400	21	8,504	591	7,913	649,811,153	58,113,193	91.34	1,949
500	43	8,504	773	7,731	660,840,001	59,099,512	91.51	1,983

Lifetime Production and Costs

In Table 17, the lifetime energy generation and capacity factor obtained from selling hydrogen is outlined, considering the addition of 100 MWp to the existing 705 MW wind farm and 650 MW Hydrogen production plant. Additionally, Table 18 provides the benefits and LCOE considering the degradation of wind, solar, and electrolyzers. Comparing Scenario 1 and Scenario 2, the addition of the FPV system increases the lifetime capacity of the 650 MW hydrogen production plant, allowing for more hours where the pipeline operates at maximum flow capacity. This means that more energy can be transported through the pipeline, resulting in a higher overall capacity for energy generation. As mentioned earlier, the demand for energy for the electrolyzer and the conversion back to electricity is halved in this scenario. This reduction in energy demand contributes to the improved overall efficiency of the system. Also, comparing the lifetime benefits to scenario 1, a same size wind farm and FPV, shows a higher profit from sold hydrogen than electricity. However, the high capital costs and lower conversion efficiency make this scenario have a higher LCOE compared to the other alternatives. This suggests that if the performance and durability of PEM electrolyzers increase, converting electricity to hydrogen could become a viable method for energy transmission, as it has the potential to significantly impact the LCOE. Similarly, the LCOE could be lower if energy transmissions, wake effect, and inter array cables, before the hydrogen production plant were not considered.

Table 17 shows the impact of lifetime energy generation including transmission losses and degradation from adding multiples of 100 MWp PV capacity to a 705 MW wind farm and a 650 MW Hydrogen production plant with a maximum pipeline capacity of 120000 nm^3

FPV Capacity (MWp)	Lifetime Energy Generation (nm^3)	Lifetime Energy Generation (kg)	Lifetime Capacity Factor (%)	Hydrogen Converted to electricity w/ LHV (GWh)
0	11,720,407,541	1,048,166,528	43.60	35,161
100	12,033,778,339	1,076,191,559	44.77	36,101
200	12,301,949,181	1,100,174,317	45.77	36,906
300	12,535,161,990	1,121,030,747	46.63	37,605
400	12,836,964,761	1,148,021,239	47.76	38,511
500	13,054,838,713	1,167,505,901	48.57	39,165

Table 18 shows the benefits and LCOE from adding multiples of 100 MWp PV capacity to a 705 MW wind farm and a 650 MW Hydrogen production plant with a maximum pipeline capacity of 120000 nm^3

FPV Capacity (MWp)	Lifetime Benefit (M€)	LCOE (€/kWh)
0	4,192.67	0.060745
100	4,304.77	0.060229
200	4,400.70	0.059959
300	4,484.12	0.059868
400	4,592.08	0.059460
500	4,670.02	0.059450

Scenario IV: 2 GW HVDC + 650 MW Hydrogen Production Plant & HPL

The following analysis describes the outcomes obtained from combining the 2 GW HVDC VSC scenario with the 650 MW Hydrogen electrolyzer production plant scenario and different sizes of FPV systems. It is important to note that the lifetime energy generation figures provided here should not be directly compared with the previous results, as they do not account for energy transmission losses. These lifetime energy generation estimates are based on the mean energy generation derived from both electricity priority and hydrogen priority data presented below. It assumed the LCOE would be higher if transmission losses were considered in this scenario.

Mean Energy Production – Electricity Priority

Figure 29 displays the total generation of the 2010 MW wind farm and 1 GWp FPV farm in comparison to the energy delivered onshore, considering cable restrictions of 2000 MWh and the conversion of excess capacity to hydrogen and back to electricity. The figure indicates that the cable capacity is frequently

reached, and although the conversion rate for green hydrogen is low, the energy gained from converting the curtailed energy to hydrogen is minimal. Table 19 and 20 illustrates the annual mean and lifetime energy generation prioritization for electricity when combining a 2010 MW offshore wind farm with a 650 MW Hydrogen PP and HPL, while considering various sizes of FPV systems in 2013. Table 21 shows the lifetime benefits and LCOE for various sizes of FPV systems.

The tables reveal that all of the curtailed energy from both the wind and FPV farms, up to a capacity of 1000 MWp, is efficiently utilized by the 650 MW hydrogen production plant. Only when the FPV system reaches a capacity of 1000 MWp does the hydrogen production plant need to curtail its output due to the maximum flow rate limitation of the hydrogen pipeline. However, it is worth noting that the hydrogen production plant's contribution to the overall energy generation is minimal, as the majority of the energy still primarily flows through the platforms and cables. The key observations from these tables are as follows: Increasing the capacity of the FPV systems leads to a more frequent utilization of the cable capacity. Therefore, the additional hydrogen production primarily stems from the integration of FPV systems. As a result, larger FPV systems have the potential to generate more energy, leading to a higher lifetime capacity for curtailed energy that is converted into hydrogen. However, the high conversion efficiency of the electrolyzers and the subsequent conversion of hydrogen back to electricity contribute only a small amount of electricity if fed back into the electrical grid.

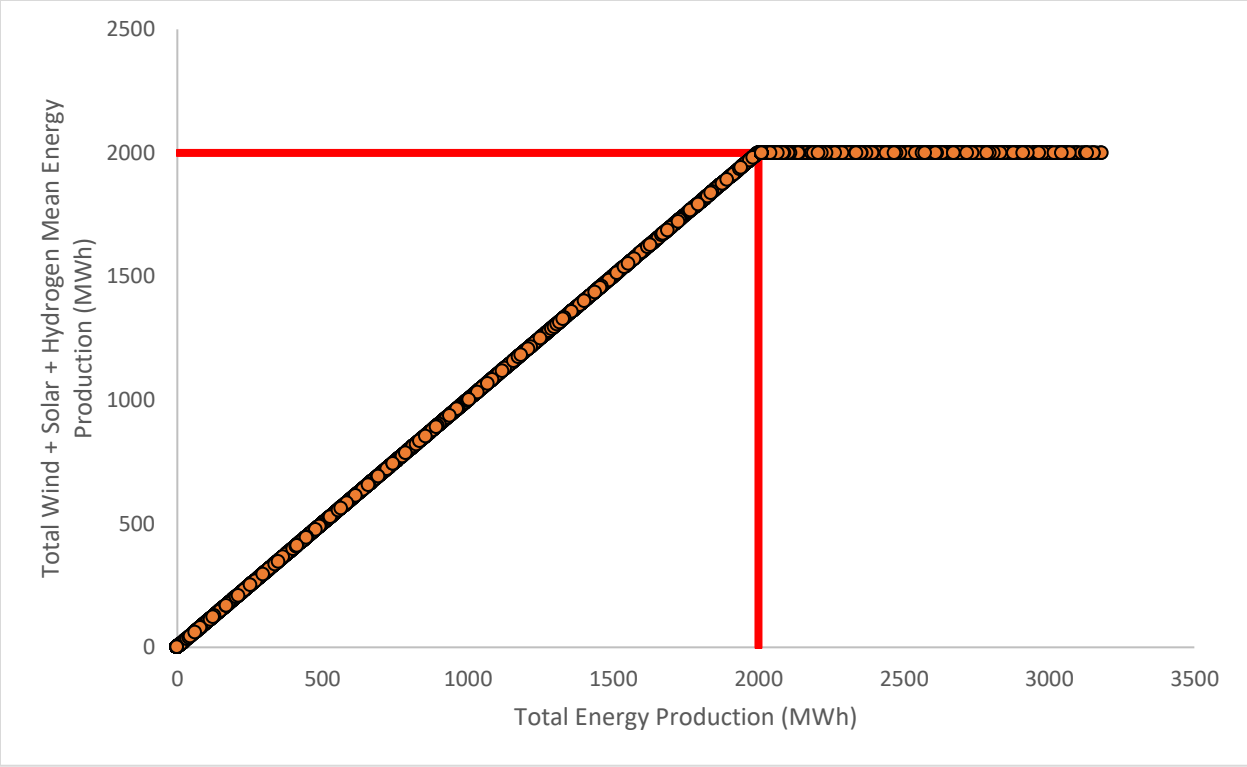

Figure 29: This scatterplot shows the correlation between 2010 MW wind farm, 1 GWp FPV farm MW energy generation, and 650 MW hydrogen production plant for "electricity priority" versus the total energy generation of the 2010 MW wind farm and 1 GWp FPV farm with red line at maximum cable capacity of 2000 MW.

Table 19 shows the impact of annual mean energy generation from adding multiples of 100 MWp PV capacity to a 2010 MW wind farm and a 650 MW Hydrogen production plant with a maximum cable capacity of 2000 MWh and pipeline capacity of 120000 nm^3 for electricity priority.

FPV Capacity (MWp)	Number of hours 2000 MWh > & > 0 nm^3	Total Energy Generation (GWh)	Mean Energy Generation (GWh)	Mean Delivered Hydrogen Onshore (nm^3)	Hydrogen Converted to electricity w/ LHV (GWh)	Curtailment Energy Converted to Hydrogen (%)	Number of hours > 120,000 nm^3
0	4,156	11,505	11,463	6,754,324	20	100	0.0
100	4,170	11,604	11,526	12,680,127	38	100	0.0
200	4,183	11,703	11,588	18,706,563	56	100	0.0
300	4,193	11,802	11,650	24,819,524	74	100	0.0
400	4,204	11,901	11,710	30,997,177	92	100	0.0
500	4,223	12,000	11,771	37,293,542	111	100	0.0
1000	4,325	12,495	12,058	69,579,103	209	97.94	9
1500	4,432	12,991	12,322	79,752,208	239	73.30	179
2000	4,534	13,486	12,560	85,175,809	256	56.57	402

Lifetime Production and Costs – Electricity Priority

Table 20 shows the impact of lifetime energy generation from adding multiples of 100 MWp PV capacity to a 2010 MW wind farm and a 650 MW Hydrogen production plant with a maximum cable capacity of 2000 MWh and pipeline capacity of 120000 nm^3 for electricity priority.

FPV Capacity (MWp)	Lifetime Energy Generation (GWh)	Lifetime Energy Generation (nm3)	Lifetime Capacity Factor Wind & Solar (%)	Lifetime Capacity Factor Hydrogen (%)
0	226,892	132,550,395	64.43	0.59
100	228,132	248,841,425	61.71	1.11
200	229,359	367,107,360	59.24	1.64
300	230,576	487,071,299	56.97	2.17
400	231,785	608,304,769	54.90	2.71
500	232,979	662,254,791	52.98	2.95
1000	238,676	1,365,456,618	45.26	6.09
1500	243,884	1,565,098,925	39.66	6.98
2000	248,605	1,671,534,498	35.39	7.46

Table 21 shows the benefits and LCOE from adding multiples of 100 MWp PV capacity to a 2010 MW wind farm and a 650 MW Hydrogen production plant with a maximum cable capacity of 2000 MWh and pipeline capacity of 120000 nm^3 for electricity priority.

FPV Capacity (MWp)	Lifetime Benefit (M€)	LCOE (€/kWh)
0	10,256.40	0.017348
100	10,359.49	0.017344
200	10,462.61	0.017340
300	10,565.74	0.017336
400	10,668.62	0.017333
500	10,747.76	0.017358
1000	11,193.66	0.017326
1500	11,494.30	0.017345
2000	11,742.07	0.017786

Mean Energy Production – Hydrogen Priority

Figure 30 presents the reverse scenario compared to Figure 29, where low total energy production results in limited available energy due to the low conversion rate. It is only when approximately 2700 MWh of generation is reached that the cable capacity starts to approach its limit in the “hydrogen priority” scenario.

Table 22 and 23 present the annual average and lifetime energy generation prioritization for hydrogen in the context of combining a 2010 MW offshore wind farm with a 650 MW Hydrogen production plant and HPL, while considering different sizes of FPV systems in 2013. Remarkably, the hydrogen plant only requires 787 MWh to operate at its maximum capacity and fill the hydrogen pipeline's maximum flow rate of 120,000 nm3/hour. Consequently, there is an abundance of energy that can be redirected to the cables for transmission onshore. The key takeaways from this analysis are twofold: First, incorporating FPV systems into the setup enhances both the capacity of hydrogen production and delivery to the onshore location, as well as increasing the cable capacity. Second, similar to the previous scenario regarding electricity priority, it is not until the FPV system reaches a capacity of 1000 MWp that curtailment of energy is necessary due to the cable reaching its maximum rated capacity. Despite the higher lifetime benefits, the LCOE is higher compared to the electricity-first scenario. This disparity can be attributed to the lower conversion efficiency of the electrolyzers employed in hydrogen production, Table 24.

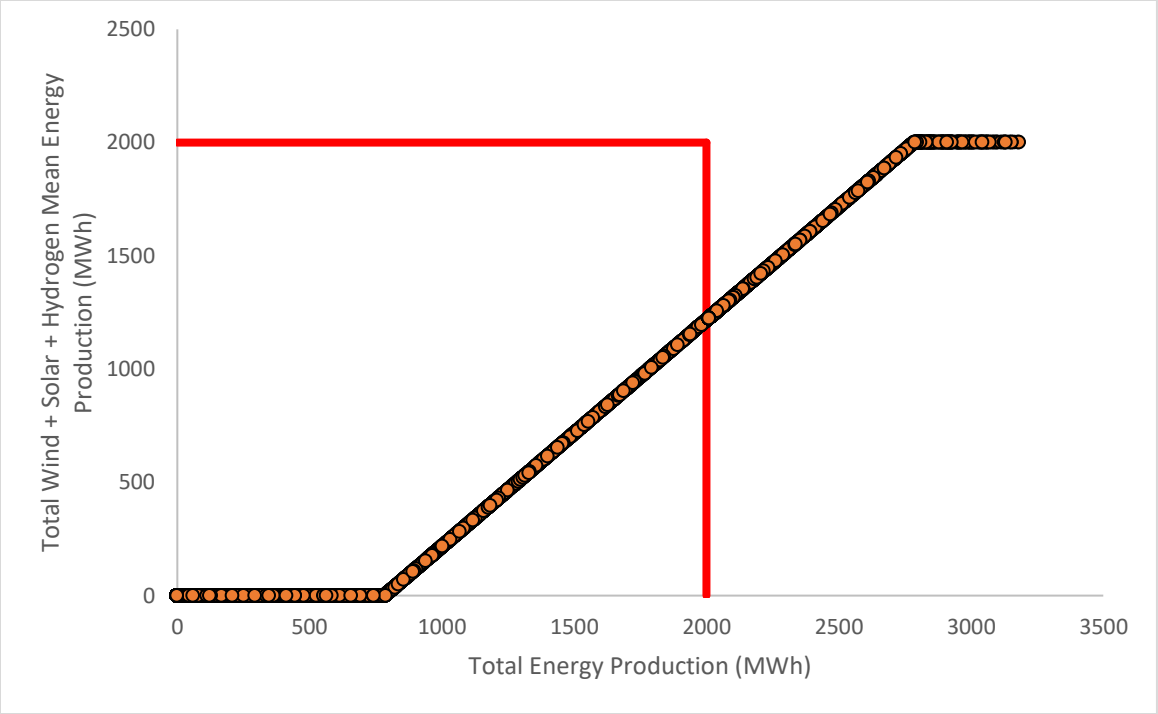

Figure 30: This scatterplot shows the correlation between 2010 MW wind farm, 1 GWp FPV farm MW energy generation, and 650 MW hydrogen production plant for "hydrogen priority" versus the total energy generation of the 2010 MW wind farm and 1 GWp FPV farm with red line at maximum cable capacity of 2000 MW.

Table 22 shows the impact of annual mean energy generation from adding multiples of 100 MWp PV capacity to a 2010 MW wind farm and a 650 MW Hydrogen production plant with a maximum cable capacity of 2000 MWh and pipeline capacity of 120000 nm^3 for hydrogen priority.

FPV Capacity (MWp)	Number of hours > 12000 nm^3 & MWh > 0	Total Hydrogen Production (nm^3)	Mean Delivered Hydrogen Onshore (nm^3)	Hydrogen Converted to electricity w/ LHV (GWh)	Mean Energy Generation (GWh)	Curtailment Energy due to Cable Capacity (%)	Number of hours > 2000 MWh
0	5,990	890,093,938	843,103,392	2,529	6,032	100	0.0
100	6,027	896,332,767	849,113,895	2,547	6,094	100	0.0
200	6,056	902,391,341	854,916,407	2,565	6,155	100	0.0
300	6084	908,253,748	860,535,936	2,582	6,218	100	0.0
400	6110	913,901,877	865,939,070	2,598	6,283	100	0.0
500	6163	919,346,147	871,055,408	2,613	6,348	100	0.0
1000	6,378	941,759,899	891,737,444	2,675	6,706	99.99	2
1500	6,589	956,253,373	904,538,990	2,714	7,088	99.66	174
2000	6,709	965,022,753	912,280,732	2,736	7,449	98.61	372

Lifetime Production and Costs – Hydrogen Priority

Table 23 shows the impact of lifetime energy generation from adding multiples of 100 MWp PV capacity to a 2010 MW wind farm and a 650 MW Hydrogen production plant with a maximum cable capacity of 2000 MWh and pipeline capacity of 120000 nm^3 for hydrogen priority.

FPV Capacity (MWp)	Lifetime Energy Generation (GWh)	Lifetime Energy Generation (nm3)	Lifetime Capacity Factor Wind & Solar (%)	Lifetime Capacity Factor Hydrogen (%)
0	165,461	16,545,500,636	33.91	73.83
100	166,991	16,663,453,887	32.62	74.35
200	168,531	16,777,325,406	31.46	74.86
300	170,085	16,887,605,967	30.41	75.35
400	171,654	16,993,639,897	29.45	75.83
500	173,232	17,094,045,578	28.57	76.27
1000	181,437	17,499,920,639	25.17	78.08
1500	189,696	17,751,144,851	22.81	79.21
2000	197,263	17,903,072,837	20.98	79.88

Table 24 shows the benefits and LCOE from adding multiples of 100 MWp PV capacity to a 2010 MW wind farm and a 650 MW Hydrogen production with a maximum cable capacity of 2000 MWh and pipeline capacity of 120000 nm^3 for hydrogen priority.

FPV Capacity (MWp)	Lifetime Benefit (M€)	LCOE (€/kWh)
0	10,865.06	0.02387
100	10,958.28	0.02384
200	11,051.13	0.02335
300	11,143.86	0.02379
400	11,236.36	0.02375
500	11,328.11	0.02372
1000	11,781.24	0.02354
1500	12,204.79	0.02336
2000	12,576.74	0.02327

B. Discussion

The objective of this research was to contribute to the existing knowledge on offshore FPV systems by evaluating the cost-effective transmission of a hybrid offshore wind and floating solar PV system to the onshore grid. The research specifically focused on the technical and economic aspects of offshore energy transmission infrastructure, aiming to maximize energy generation and transmission efficiency while minimizing infrastructure costs for the integration of these two renewable systems. By applying the most cost-efficient approach in the future planning of the Doordewind Wind Farm Zone, this research has the potential to impact energy generation availability and contribute to a more secure energy supply in the Netherlands' transition to renewable energy sources.

The 2 GW HVDC VSC transmission system is identified as the best cost-efficient method to transport energy from offshore wind and FPV when only examining singular transmission methods. As this technology is going to be applied in the coming years for the next wind farm tender, adding FPV systems can help maximize the energy generation of the transmission capacity and additional benefits. But this integration also brings about an increase in the levelized costs with added transmission system components. One of the main limitations associated with combining wind and solar energy in a hybrid offshore system is the increased curtailment of both sources, resulting in higher energy losses. Additionally, the 2010 MW wind farm is susceptible to higher energy losses due to the wake effect. Furthermore, the HVDC conversion stations tend to have higher energy losses compared to HVAC substations. In addition to the HVDC VSC option, the research also identified the 700 MW HVAC system as the second-best alternative. This system was found to effectively double the onshore energy availability compared to the 650 MW hydrogen production plant option. Besides, the LCOE for the 700 MW HVAC was determined to be approximately three times lower than that of the 650 MW hydrogen production plant option. Contrarily, the research findings indicated that the 650 MW hydrogen production plant yielded greater benefits over its lifetime. This outcome can primarily be attributed to the higher capacity rate and the size of the pipeline utilized in comparison to submarine cables. The increased capacity rate of the hydrogen production plant, coupled with the larger pipeline, led to enhanced cost-effectiveness throughout the lifespan of the system. Thus, the 650 MW hydrogen production plant demonstrated performance advantages regarding the pipeline. But the LCOE associated with the 650 MW hydrogen production plant could potentially decrease in the future through rapid technological advancements in PEM electrolyzers, leading to improved conversion efficiencies

and lowered costs. These anticipated advancements highlight the potential for even greater cost-efficiency and improved economic viability of the 650 MW hydrogen production plant option in the future.

When considering Scenario 4, where the operational priority is given to both electricity and hydrogen, it becomes evident that the electricity priority is the preferable transmission method. The integration of FPV significantly increases the operational frequency of the transmission system and the 650 MW hydrogen production plant. When adding FPV systems, this mainly supports generation to the hydrogen production plant, especially when the wind farm is operating at maximum capacity and the cable is fully utilized. However, the cumulative capacity of FPV systems over 1 GWp start to exceed the pipeline's capacity, and curtailment of the hydrogen production plant occurs. Nevertheless, Scenario 4 offers substantial benefits compared to the hydrogen priority as annual and lifetime generation is nearly doubled. Additionally, it demonstrates a lower LCOE, but similarly to scenario 3, the lifetime benefits are more substantial in the hydrogen scenario, as the pipeline is maximized more frequently, resulting in increased hydrogen transmission onshore throughout its operational lifespan. Moreover, the scenario's viability can be further enhanced if the cost and efficiency of PEM technology improve. This can be attributed to the potential rise in overall demand for hydrogen and advancements in PEM technology, leading to further cost reductions.

In the present and anticipated future market, there is an evident and increasing demand for hydrogen, particularly in industries with hard to abate carbon emissions. Although it is important to consider the utilization of hydrogen as a means to mitigate energy curtailment in offshore wind and FPV production when the capacity of cables is being reached. Green hydrogen should also be an energy carrier for transporting and storing renewable energy during periods of low demand or price. Leveraging existing infrastructure and expertise from natural gas usage, pipelines have the potential to transport substantial amounts of affordable renewable energy from regions with high production to areas with high energy demand. During the interviews, many experts highlighted the progress in offshore wind technology, which has transitioned from being expensive and heavily subsidized a decade ago to becoming subsidy-free today. They expressed similar optimism for offshore FPV and green hydrogen technologies. In addition, the offshore renewable industry has demonstrated high levels of competitiveness, especially with the upcoming large wind farm tenders in the next few years. Major renewable energy developers have been collaborating with offshore FPV and hydrogen companies, forming strategic partnerships to meet the Dutch government's needs and showcasing high-capacity rates for future wind tenders. The

Dutch government considers the cost of grid connection for offshore wind farms as a social cost. The government supports the costs associated with grid connection for renewable developers, aiming to promote and facilitate offshore energy generation. However, these renewable developers primarily prioritize their shareholders' interests rather than serving the general public. To address this, there is a need for the creation of private-public partnerships that not only provide affordable clean energy access to the public but also allow them to participate in the profits. Currently, these services are often dominated by private companies, with limited benefits reaching the general public. Similar partnerships have been established between renewable energy developers and renewable energy cooperatives, enabling members to earn profits while also generating economic, environmental, and social benefits for both members and society. As the renewable energy industry rapidly evolves, governments and stakeholders are actively pursuing leadership in this transition. Although, since the public bears the consequences of these actions, they should have a greater stake and voice in the decision-making processes. In the end, all available transmission methods should be considered in tenders and road maps even as the benefits derived from various transmission systems can outweigh the associated additional costs.

Limitations

The presented results should be taken theoretically, as the construction and operation of offshore renewables typically involve substantial uncertainties and risks. Real-world implementation may introduce additional factors and challenges that could impact the viability of these offshore renewable energy systems. The analysis did not incorporate specific environmental conditions, which can significantly impact the energy generation of these systems. As offshore renewable projects continue to progress, new information emerges daily, causing much of the available information to quickly become outdated. Also, extra electrical infrastructures such as storage were not considered in this analysis. The scenarios assume that all the energy and hydrogen brought onshore will have a designated use. However, in practice, the costs and implementation of storage systems should be evaluated, as this can have a role in the efficiency and economic feasibility of the hybrid offshore wind, FPV, and hydrogen system. Lastly, while this analysis focuses on the North Sea, there may be more suitable locations for deploying hybrid offshore wind, FPV, and hydrogen systems. Different geographical areas may offer advantageous conditions in terms of resource availability in wind and solar, weather, and infrastructure proximity. Therefore, site assessments should consider locational

factors when planning and implementing such hybrid systems in order to maximize their effectiveness and potential benefits.

Future Research

Future research in offshore renewable energy development should prioritize investigating the environmental impacts associated with the integration of offshore wind, FPV, and hydrogen systems in the North Sea. As FPV and hydrogen technologies are still relatively new, there are many unknowns regarding long term performance and environmental impacts in offshore conditions. Ongoing pilot projects are currently underway, and once these pilot projects are completed having access to valid data and information will be crucial for future academic research. This data then can be used to understand the environmental implications of combining these three systems. It will help researchers evaluate potential effects on marine ecosystems, wildlife, and water quality. Conducting thorough environmental assessments will facilitate the quicker and more responsible development of hybrid offshore systems.

4. Conclusion

In conclusion, the fast-growing need to transition the energy sector towards renewable sources in the Netherlands, driven by EU climate targets, has resulted in extensive growth of renewable energy development, particularly in PV and wind technologies. Based on the literature review and interviews with the energy and cost modeling, this paper identifies the 2 GW HVDC VSC, and the electricity priority determined to be the best options because these scenarios were able to maximize the energy generation and transmission in a cost-effective manner. Depending on the advancements in hydrogen technologies and changes in the market, it may could make using the pipeline could become a more viable cost-efficient option in the future. It is recommended to explore and utilize all available options as they contribute to enhanced energy security and stability. However, implementing diverse transmission options will occur higher costs. Nonetheless, the benefits of increased energy security could outweigh the financial implications, ensuring a more reliable energy system.

Bibliography

1. Andrews, J., & Jelley, N. (2022). *Energy science principles, technologies, and impacts*. Oxford University Press.
2. Ansari, D., Grinschgl, J., & Pepe, J. M. (2022). Electrolysers for the hydrogen revolution - swp-berlin.org. https://www.swp-berlin.org/publications/products/comments/2022C57_Electrolysers_HydrogenRevolution.pdf
3. Ansari, D., Grinschgl, J., & Pepe, J. M. (2022). Electrolysers for the hydrogen revolution - swp-berlin.org. https://www.swp-berlin.org/publications/products/comments/2022C57_Electrolysers_HydrogenRevolution.pdf
4. Aurora Energy Research. (2022). *Shades of green (hydrogen) – part 2: in pursuit of 2 EUR/kg*. Aurora Energy Research. https://www.provinciegroningen.nl/fileadmin/user_upload/Documenten/Beleid_en_documenten/Documentenzoeker/Klimaat_en_energie/Energie_transitie/Nieuwe-energie-voor-Groningen.pdf
5. Badgett, A., Ruth, M., & Pivovar, B. (2021). Economic considerations for hydrogen production with a focus on polymer electrolyte membrane electrolysis. In *Electrochemical Power Sources: Fundamentals, Systems, and Applications Hydrogen Production by Water Electrolysis*. https://doi.org/10.1016/B978-0-12-819424-9.00005-7
6. BBL Company, (2023). Balgzand Bacton Line, BBL . *About BBL*. https://www.bblcompany.com/about-bbl
7. Breunis, W. (2021). *Hydrogen gas production from Offshore Wind: A cost-benefit analysis of optionality through grid connection*. TU Delft Repositories. https://repository.tudelft.nl/islandora/object/uuid%3A592c4ab2-7ab1-428b-b54c-1c44afc5ba5a
8. Caglayan, D. G., Weber, N., Heinrichs, H. U., Linßen, J., Robinius, M., Kukla, P. A., & Stolten, D. (2020). Technical potential of salt caverns for hydrogen storage in Europe. *International Journal of Hydrogen Energy*, *45*(11). https://doi.org/10.1016/j.ijhydene.2019.12.161
9. Carton, J. G., & Olabi, A. G. (2010). Wind/hydrogen hybrid systems: Opportunity for Ireland's wind resource to provide consistent sustainable energy supply. *Energy*, *35*(12). https://doi.org/10.1016/j.energy.2010.09.010
10. CASFHPU, Committee on Alternatives and Strategies for Future Hydrogen Production and Use. (2004) The Hydrogen Economy: Opportunities, Costs, Barriers, and R&D Needs. United States. https://doi.org/10.2172/882095
11. CBS. (2021). *Three-quarters of Dutch concerned about impact of climate change*. Statistics Netherlands. https://www.cbs.nl/en-gb/news/2021/22/three-quarters-of-dutch-concerned-about-impact-of-climate-change
12. Chi, J., & Yu, H. (2018). Water electrolysis based on renewable energy for hydrogen production. In *Cuihua Xuebao/Chinese Journal of Catalysis* (Vol. 39, Issue 3). https://doi.org/10.1016/S1872-2067(17)62949-8
13. Christensen, A. (2020). Assessment of Hydrogen Production Costs from Electrolysis: United States and Europe. In *International Council on Clean Transportation (ICCT)*.
14. Dame, S. (2022). *SolarDuck awarded the world´s largest hybrid offshore floating solar power plant at the offshore wind park Hollandse Kust West VII (Netherlands), following winning bid of RWE´s subsidiary Oranje Wind Power II*. https://solarduck.tech/wp-content/uploads/2022/11/SolarDuck-Press-release-HKW-VII-Nov-11-2022-v1.pdf
15. DOE. (2022). *Hydrogen production: Electrolysis*. Energy.gov. Retrieved March 10, 2023, from https://www.energy.gov/eere/fuelcells/hydrogen-production-electrolysis
16. Enbar, N., Weng, D., & Klise, G. T. (2015). *Budgeting for solar PV Plant Operations & Maintenance: Practices and pricing.* Budgeting for Solar PV Plant Operations & Maintenance: Practices and Pricing. (Technical Report) | OSTI.GOV. https://www.osti.gov/servlets/purl/1234935
17. EU Commisson. (2023). *Supporting clean hydrogen*. Internal Market, Industry, Entrepreneurship and SMEs. https://single-market-economy.ec.europa.eu/industry/strategy/hydrogen_en#:~:text=Hydrogen%20is%20expected%20to%20play,to%20contribute%20to%20climate%20neutrality.
18. Fernández-Guillamón, A., Das, K., Cutululis, N. A., & Molina-García, Á. (2019). Offshore wind power integration into future power systems: Overview and trends. *Journal of Marine Science and Engineering*, *7*(11). https://doi.org/10.3390/jmse7110399
19. Findlay, C. (2020). *Repurposing gas pipelines for Hydrogen*. What's your purpose? Reusing gas infrastructure for hydrogen transportation. https://www.siemens-energy.com/global/en/news/magazine/2020/repurposing-natural-gas-infrastructure-for-hydrogen.html
20. Folkers, W., van Sark, W., de Keizer, C., van Hooff, W., & van den Donker, M. (2017). Roadmap pv systems and applications. Study commissioned by the Netherland s Enterprise Agency (RVO) in collaboration with the TKI Urban. Energy.
21. Gaertner, Evan, Jennifer Rinker, Latha Sethuraman, Frederik Zahle, Benjamin Anderson, Garrett Barter, Nikhar Abbas, Fanzhong Meng, Pietro Bortolotti, Witold Skrzypinski, George Scott, Roland Feil, Henrik Bredmose, Katherine Dykes, Matt Shields, Christopher Allen, and Anthony Viselli. 2020. Definition of the IEA 15-Megawatt Offshore Reference Wind. Golden, CO: National Renewable Energy Laboratory. NREL/TP-5000-75698. https://www.nrel.gov/docs/fy20osti/75698.pdf
22. Gasunie. (2020). *Europe's largest green hydrogen project starts in Groningen*. https://www.gasunie.nl/en/news/europes-largest-green-hydrogen-project-starts-in-groningen

23. Gigler, J., Koole , D., & Blekxtoon, J. (2022). *Excelling in Hydrogen Dutch technology for a climate-neutral world*. NL Dutch solutions for a hydrogen economy. https://english.rvo.nl/sites/default/files/2022/05/NL-Dutch-solutions-for-a-hydrogen-economy-V-April-2022-DIGI_0.pdf
24. Golroodbari, S. Z. M., Vaartjes, D. F., Meit, J. B. L., van Hoeken, A. P., Eberveld, M., Jonker, H., & van Sark, W. G. J. H. M. (2021). Pooling the cable: A techno-economic feasibility study of integrating offshore floating photovoltaic solar technology within an offshore wind park. *Solar Energy*, *219*. https://doi.org/10.1016/j.solener.2020.12.062
25. Golroodbari, S. Z., Ayyad, A. W. A., & van Sark, W. (2023, June 20). *Offshore floating photovoltaics system assessment in worldwide perspective*. Progress in Photovoltaics. https://onlinelibrary.wiley.com/doi/10.1002/pip.3723#pane-pcw-references
26. Gorjian, S., Sharon, H., Ebadi, H., Kant, K., Scavo, F. B., & Tina, G. M. (2021). Recent technical advancements, economics and environmental impacts of floating photovoltaic solar energy conversion systems. *Journal of Cleaner Production*, *278*, 124285. https://doi.org/10.1016/J.JCLEPRO.2020.124285
27. Grigoriev, S. A., Dzhus, K. A., Bessarabov, D. G., & Millet, P. (2014). Failure of PEM water electrolysis cells: Case study involving anode dissolution and membrane thinning. *International Journal of Hydrogen Energy*, *39*(35). https://doi.org/10.1016/j.ijhydene.2014.05.043
28. Guo, Y., Li, G., Zhou, J., & Liu, Y. (2019). Comparison between hydrogen production by alkaline water electrolysis and hydrogen production by PEM electrolysis. *IOP Conference Series: Earth and Environmental Science*, *371*(4). https://doi.org/10.1088/1755-1315/371/4/042022
29. Hou, P., Enevoldsen, P., Eichman, J., Hu, W., Jacobson, M. Z., & Chen, Z. (2017). Optimizing investments in coupled offshore wind electrolytic hydrogen storage systems in Denmark. *Journal of Power Sources*, *359*. https://doi.org/10.1016/j.jpowsour.2017.05.048
30. Iberdrola. (2021). *What is an electrolyser and why is it key to green hydrogen supply?*. Iberdrola. https://www.iberdrola.com/sustainability/electrolyzer#:~:text=The%20oxygen%20generated%20in%20parallel,trains%2C%20ships%20and%20even%20aircraft.
31. IEA (2021), Net Zero by 2050, IEA, Paris https://www.iea.org/reports/net-zero-by-2050, License: CC BY 4.0
32. IEA, (2020) Netherlands solar PV capacity additions, 2018-2022 and average annual additions, 2023-2025, IEA, Paris https://www.iea.org/data-and-statistics/charts/netherlands-solar-pv-capacity-additions-2018-2022-and-average-annual-additions-2023-2025, IEA. Licence: CC BY 4.0
33. IRENA (2022). *Innovation trends in electrolysers for hydrogen production*. Patent insight report. Retrieved March 13, 2023, from https://www.irena.org/-/media/Files/IRENA/Agency/Publication/2022/May/IRENA_EPO_Electrolysers_H2_production_2022.pdf?rev=647d930910884e51b60137bcf5a955a6
34. Jordan, D. C., & Kurtz, S. R. (2012). Photovoltaic degradation risk (No. NREL/CP-5200-53712). National Renewable Energy Lab.(NREL), Golden, CO (United States).
35. Kallio H, Pietilä AM, Johnson M, Kangasniemi M. (2016 Dec) Systematic methodological review: developing a framework for a qualitative semi-structured interview guide. J Adv Nurs.;72(12):2954-2965. doi: 10.1111/jan.13031. Epub 2016 Jun 23. PMID: 27221824.
36. Keddar, M., Da Conceicao, M., Doumbia, M., & Zhang, Z. (2022). *Electrolyzer degradation-power electronics one -way interaction model*. Applied Energy Symposium: MIT A+B. https://www.energy-proceedings.org/wp-content/uploads/2022/08/MITAB_2022_paper_6450.pdf
37. Keith, G., & Leighty, W. (2002). Transmitting 4,000 mw of new windpower from north Dakota to Chicago: New HVDC electric lines or hydrogen pipeline. *40th AIAA Aerospace Sciences Meeting and Exhibit*. https://doi.org/10.1109/pess.2002.1043288
38. Knol, E. & Coolen, E. (2019). Employment analysis (2019-2023) of various fields of activities in the Dutch offshore wind sector. Study commissioned by RVO (Netherlands Enterprise Agency) and TKI Wind op Zee.
39. Kratzenberg, M. G., Deschamps, E. M., Nascimento, L., Rüther, R., & Zürn, H. H. (2014). Optimal photovoltaic inverter sizing considering different climate conditions and energy prices. *Energy Procedia*, *57*. https://doi.org/10.1016/j.egypro.2014.10.027
40. Kuczynski, S., Łaciak, M., Olijnyk, A., Szurlej, A., & Włodek, T. (2019). Thermodynamic and technical issues of hydrogen and methane-hydrogen mixtures pipeline transmission. *Energies*, *12*(3). https://doi.org/10.3390/en12030569
41. Kumar, S., & Himabindu, V. (2019). Hydrogen production by PEM water electrolysis – A review. In *Materials Science for Energy Technologies* (Vol. 2, Issue 3). https://doi.org/10.1016/j.mset.2019.03.002
42. Lazaridis, L. P. (2005). Economic comparison of HVAC and HVDC solutions for large offshore wind farms under special consideration of reliability. In *Master½s Thesis X{#} ETS/ESS*.
43. Mahajan, D., Tan, K., Venkatesh, T., Kileti, P., & Clayton, C. R. (2022). Hydrogen Blending in Gas Pipeline Networks—A Review. In *Energies* (Vol. 15, Issue 10). https://doi.org/10.3390/en15103582
44. Muhammad, A., Muhammad, U., & Abid, Z. (2021). Potential of floating photovoltaic technology in Pakistan. *Sustainable Energy Technologies and Assessments*, *43*, 100976. https://doi.org/10.1016/J.SETA.2020.100976
45. NASA. (2023). *NASA POWER*. NASA. https://power.larc.nasa.gov/
46. Negra, N. B., Todorovic, J., & Ackermann, T. (2006). Loss evaluation of HVAC and HVDC transmission solutions for large offshore wind farms. *Electric Power Systems Research*, *76*(11). https://doi.org/10.1016/j.epsr.2005.11.00

47. Nel. (2023). *M Series Containerized PEM Electrolysers*. https://nelhydrogen.com/wp-content/uploads/2021/01/M-Series-Containerized-Spec-Sheet-Rev-F.pdf
48. Noordzeeloket NL. (2023). *Offshore Wind Energy Roadmap with cable routes from the offshore grid*. https://www.noordzeeloket.nl/en/functions-and-use/offshore-wind-energy/offshore-grid/
49. Ramasamy, V, and Robert, M. (2021). Floating Photovoltaic System Cost Benchmark: Q1 2021 Installations on Artificial Water Bodies. Golden, CO: National Renewable Energy Laboratory. NREL/TP-7A40-80695. https://www.nrel.gov/docs/fy22osti/80695.pdf.
50. Reich, N. H., Mueller, B., Armbruster, A., van Sark, W. G. J. H. M., Kiefer, K., & Reise, C. (2012). Performance ratio revisited: Is PR > 90% realistic? *Progress in Photovoltaics: Research and Applications*, *20*(6). https://doi.org/10.1002/pip.1219
51. Ruijgrok, E.C.M., van Druten, E.J., Bulder, B.H., and van Kuijk, A.H.J.. (2019, February) North Sea Wind Power Hub, Cost evaluation of North Sea offshore wind post 2030. https://northseawindpowerhub.eu/ cost-evaluation-of-north-sea-offshore-wind-post-2030-towards-spatial-planning/
52. RVO. (2022). *Development framework for offshore wind energy* . https://english.rvo.nl/sites/default/files/2022/07/Development-Framework-Offshore-Wind-Energy-June-2022.pdf
53. RWE. (2022). *Eemshydrogen*. https://www.rwe.com/en/research-and development/hydrogen-projects/eemshydrogen/
54. Sahu, A., Yadav, N., & Sudhakar, K. (2016). Floating photovoltaic power plant: A review. In Renewable and Sustainable Energy Reviews (Vol. 66). https://doi.org/10.1016/j.rser.2016.08.051
55. Shawn. (2013). *Most-efficient-solar-inverters*. SRoeCo Solar. http://sroeco.com/solar/most-efficient-solar-inverters/
56. Siemens . (2023). *Israel's largest floating photovoltaic plant supplied with Siemens' Inverter Technology*. https://www.siemens.com/us/en/products/energy/medium-voltage/photovoltaic-inverters/largest-floating-pv-plant-with-siemens-inverters.html
57. Singlitico, A., Østergaard, J., & Chatzivasileiadis, S. (2021). Onshore, offshore or in-turbine electrolysis? Techno-economic overview of alternative integration designs for green hydrogen production into Offshore Wind Power Hubs. *Renewable and Sustainable Energy Transition*, *1*. https://doi.org/10.1016/j.rset.2021.100005
58. Solar Energy Research Institute of Singapore (SERIS), & National University of Singapore. (NUS) (2019). *Where sun meets water – World Bank*. https://openknowledge.worldbank.org/bitstream/handle/10986/31880/Floating-Solar-Market-Report.pdf
59. Staffell, I., & Green, R. (2014). How does wind farm performance decline with age?. *Renewable energy*, *66*, 775-786.
60. Sungrow. (2020). *SG250HX*. https://en.sungrowpower.com/upload/file/20210108/DS_20201121_SG250HX%20Datasheet_V1.5.4_EN.pdf.pdf
61. Taieb, A., & Shaaban, M. (2019). Cost Analysis of Electricity Transmission from Offshore Wind Farm by HVDC and Hydrogen Pipeline Systems. *2019 IEEE PES GTD Grand International Conference and Exposition Asia, GTD Asia 2019*, 632–636. https://doi.org/10.1109/GTDASIA.2019.8715900
62. TenneT. (2016). *Kwaliteits- en Capaciteitsdocument*. TenneT. https://netztransparenz.tennet.eu/fileadmin/user_upload/Company/Publications/Technical_Publications/Dutch/TP_KCD2016_net_op_zee.pdf
63. TenneT. (2022). *Offshore projects netherlands*. TenneT. https://www.tennet.eu/projects/offshore-projects-netherlands
64. TenneT. (2023). *The 2GW program - More wind energy for Europe*. TenneT. https://www.tennet.eu/our-grid/offshore-outlook-2050/the-2gw-program
65. TNO. (2022). *Scenarios for a climate-neutral energy system for the Netherlands*. Impact of the energy transition. Retrieved from https://www.tno.nl/nl/newsroom/2022/04/ambitieuze-scenario-klimaatneutraal/
66. TSC. (2022). *TSC PowerXT | DC Panel*. https://static1.squarespace.com/static/5fa44724b1ca66220ca21c60/t/62215c0716614538b33ee5bb/1646353417082/Datasheet_TSC_PowerXT_TSC_Resi-400PM.pdf
67. Vairavasundaram, I., Varadarajan, V., Pavankumar, P. J., Kanagavel, R. K., Ravi, L., & Vairavasundaram, S. (2021). A Review on Small Power Rating PV Inverter Topologies and Smart PV Inverters. *Electronics*, *10*(11), 1296. https://doi.org/10.3390/electronics10111296
68. van den Brink, M., Olijve, N., & Pustjens, W. (2020). *Determination of the cost levels of wind farms (and their grid connections) in new offshore wind energy search areas*. BLIX Consultancy BV & partners. https://www.commissiemer.nl/projectdocumenten/00009966.pdf
69. Van Eeckhout, B., Van Hertem, D., Reza, M., Srivastava, K., & Belmans, R. (2009). *Economic comparison of VSC HVDC and HVAC as transmission system for a 300 MW offshore wind farm*. EUROPEAN TRANSACTIONS ON ELECTRICAL POWER. https://www.researchgate.net/publication/228055724_Economic_comparison_of_VSC_HVDC_and_HVAC_as_transmission_system_for_a_300MW_offshore_wind_farm
70. Vestas Wind Systems A/S. (2023). *V236-15.0 MW™ IEC S or S,T; Facts&Figures https://www.vestas.com/en/products/offshore/V236-15MW*
71. Vignola, F., Krumsick, J., & Mavromatakis, F. (2004). Performance of PV inverters . http://solardat.uoregon.edu/download/Papers/PerformanceofPVInverters.pdf

72. Vis, J. (2020). *Netwerk op zee & North Sea Wind Power Hub*. TenneT. https://www.kivi.nl/uploads/media/5fc7767d73a59/20201201%20Netwerk%20op%20zee%20&%20Noth%20Sea%20Wind%20Power%20Hub%20Jasper%20Vis%20Tennet%20%20KIVI%20Jaarcongres.pdf
73. Wang, H., Zhao, X., Zhang, K., & Wang, W. (2022). Economic assessment of a renewable energy-electricity-hydrogen system considering environmental benefits. *Sustainable Production and Consumption*, *33*. https://doi.org/10.1016/j.spc.2022.08.010
74. Weichenhain, U., Elsen, S., Zorn, T., Kern, S., (2019). *Hybrid projects : how to reduce costs and space of offshore developments, North seas offshore energy cluste*rs studyDoi:, doi:10.2833/416539.
75. Wijnant, I. L., van den Brink, H. W., Savenije, M., & Stepek, A. (2016, June). User manual of the (KNMI North Sea Wind) KNW-Atlas. https://www.knmiprojects.nl/binaries/knmiprojects/documenten/reports/2016/06/01/knw-user-manual/KNW+Atlas_User+manual-versie9.pdf
76. WWW, windandwaterworks.nl. (2023). *Dutch Offshore Wind Innovation Guide: Your guide to Dutch offshore wind policy, technologies and innovations*. RVO. https://www.rvo.nl/sites/default/files/2022-11/Dutch-offshore-Wind-Innovation-Guide-Edition-2023.pdf

Appendix

Appendix A – Interviewees, Transcripts, and Interview Guide

Interview	Profession	Date
1	Business Development Manager – Fred Olsen	31-03-2023
2	Department of Solar Energy – TNO	06-04-2023
3	Department of Renewable Energy Road Map & System Integration – TNO	12-04-2023
4	Professor in Future Energy Systems – TU Delft	26-04-2023
5	Business Development Manager – Oceans of Energy	08-05-2023
6	Lead System Integrator - Crosswind	09-04-2023

Google Link for Transcripts: https://docs.google.com/document/d/1zIZMJkXyNWV-Q7sFxIx_4YBbkGC4HEzTJTj14Q8d_HM/edit?usp=sharing

Introduction

I am currently a master's student at Utrecht University researching transmission methods for offshore floating PV in combination with offshore wind in the North Sea. The focus of the research is to examine the energetic and economic effects of offshore FPV and wind on the planned substation and cables. As well as alternatively the effects of transmitting offshore FPV and wind by converting to green hydrogen. The main purpose is to determine the optimal method for transmission to maximize the generation and transmission efficiency and minimize costs considering the planned designs for electrical transmission infrastructure.

Disclaimer

May I use your name and function in my research? Is it okay if I record the interview? Please let me know if you have problem with either and if you have any questions before we start. The interview will take about half an hour and has about 8 questions.

Introduction

What is your name?

What is your position and role at X?

Technical FPV

What is the optimal electrical layout for large scale offshore FPV systems? Specifically looking at platform/inverters and cables.

- Are the inverters string or centralized? Are they located onshore or offshore?
- Similar with the cables, are they floating, grounded, or buried? Dynamic cables?
- If you can, what specifically inverters and cables are being used?

What are the energetic and economic advantages and limitations of the electrical layout X has selected?

- Performance and durability of the components?
- How often do these components to maintenance or need to be replaced?
- Costs, Budget, Subsides?
- Knowledge and technology readiness?

What is X doing to overcome these limitations for transporting offshore FPV electricity?

Technical FPV + Wind + Hydrogen

Has X researched combining offshore FPV systems with offshore wind? If so, does your preferable electrical layout stay the same or change? If not, how do you plan on connecting offshore FPV to onshore? Similar questions with combining offshore FPV systems with electrolysers for green hydrogen?

In your opinion, what is the primary obstacle preventing large scale offshore FPV development? A few possibilities: costs, technology, durability of components, supply chain logistics, design of system.

What is the current state of the hydrogen market in the Netherlands, and what are the future opportunities for green hydrogen production? What will trigger this larger demand of hydrogen in the future?

What are the main challenges and barriers to the development of green hydrogen in the Netherlands, such as technological, regulatory, and infrastructure-related challenges?

What are the key considerations for investors and companies in evaluating the business case for green hydrogen projects in the Netherlands, including financial viability, return on investment, and risk management?

What are the existing and potential policies, incentives, and regulations that can support the business case for green hydrogen in the Netherlands, and what are the risks associated with these policies?

Is there one collaboration and partnerships between the government, private sector, and other stakeholders that can accelerate the adoption of green hydrogen in the Netherlands?

Appendix B: Vestas Data Sheet

Power regulation	Pitch regulated with variable speed
Operating data	
Rated power	15,000kW
Cut-in wind speed	3m/s
Cut-out wind speed	31m/s
Wind class	IEC S or S,T
Standard operating temperature range from -10°C to +23°C* with a de-rating interval from +23°C to +45°C	
*High ambient temperature variant available	
Sound power	
Maximum	115.3dB(A)
Rotor	
Rotor diameter	236m
Swept area	43,742m²
Aerodynamic brake	three blades full feathering
Electrical	
Frequency	50/60Hz
Converter	full scale
Gearbox	
Type	medium speed
Tower	
Hub heights	site-specific

Appendix C: TSC – Solar Panel Data Sheet

TSC®

PowerXT®-400R-PM

Performance at STC (1000W/m², 25° C, AM 1.5)

PowerXT-		400R-PM
Max Power (P_{max})*	[W]	400
Efficiency	[%]	20.2
Open Circuit Voltage (V_{oc})*	[V]	51.68
Short Circuit Current (I_{sc})*	[A]	9.97
Max Power Voltage (V_{mp})	[V]	43.08
Max Power Current (I_{mp})	[A]	9.28
Power Range	[W]	-0/+5

* Measurement Tolerance Pmax +/-3%, Tolerance Voc +/- 2%, Tolerance Isc +/- 4%

Performance at NOCT (800W/m², 20°C Amb, Wind 1 m/s, AM 1.5)

Max Power (Pmax)	[W]	294.2
Open Circuit Voltage (V_{oc})	[V]	47.73
Short Circuit Current (I_{sc})	[A]	8.05
Max Power Voltage (V_{mp})	[V]	39.22
Max Power Current (I_{mp})	[A]	7.50

Temperature Characteristics

NOCT	[°C]	45 +/-2
Temp. Coeff. of P_{max}	[% / °C]	-0.39
Temp. Coeff. of V_{oc}	[% / °C]	-0.29
Temp. Coeff. of Isc	[% / °C]	0.04

Design Parameters

Operating temperature	[°C]	-40 to +85
Max System Voltage	[V]	1000
Max Fuse Rating	[A]	20
Bypass Diodes	[#]	4

IV Curves vs. Irradiance (400W Panel)

Mechanical Characteristics

Cell Type	Monocrystalline Silicon
Dimensions (L x W x H)	1644mm x 1204mm x 40mm 64.7" x 47.4" x 1.6"
Weight	21 kg
Glass Type / Thickness	AR Coated, Tempered / 2.8mm
Frame Type	Black Anodized Aluminum
Cable Type / Length	PV Wire / 1000mm
Connector Type	MC4
Junction Box	IP68 / 4 diodes
Front Load	5400 Pa*
Rear Load	3600 Pa*

*Refer to Installation Manual for details

Certifications / Test / Warranty

Certifications	IEC 61215/61730 (Ed. 2016)
Fire Type, UL 1703 (US)	Type 1
Fire Class, UIA 9174 (Italy)	Class 1
Safety Class	IEC 61140, Class II
PID Test	IEC 62804
Salt Mist	IEC 60701
Power, Parts & Labor Warranty	30 years*

* Warranty details at www.solaria.com/europe

Packaging

Stacking Method	Horizontal / Palletized
Panels/ Pallet	25
Pallet Dims (L x W x H)	67.7" x 49.6" x 49.1" 1720mm x 1260mm x 1246mm
Pallet Weight	575 kg
Pallets / 40-ft Container	18
Panels / 40-ft Container	450

Appendix D: Nel MC500 Containerized PEM Electrolyzers

MODEL	MC250	MC500
Class	1.25 MW	2.5 MW
Description	Fully-automated MW-class on-site hydrogen generator utilizing a modular containerized design for ease of installation and integration Tri-mode operation (selectable): • Command mode allows operation based on customer input current command • Load following mode automatically adjusts output to match demand • Tank filling mode operates with power-conservation mode during standby	
Electrolyte	Proton Exchange Membrane (PEM) – caustic-free	
HYDROGEN PRODUCTION		
Nominal Production Rate Nm^3/h @ 0° C, 1 bar SCF/h @ 70° F, 1 atm kg/24 h	246 Nm^3/h 9,352 SCF/h 531 kg/24 h	492 Nm^3/h 18,704 SCF/h 1,062 kg/24 h
Delivery Pressure – Nominal	30 barg (435 psig); full differential pressure H_2 over O_2	
Power Consumption at Stack per Volume of H_2 Gas Produced at 100% capacity[1]	4.7 kWh/Nm^3	
Power Consumption at System per Volume of H_2 Gas Produced at 100% capacity[1]	5.1 kWh/Nm^3	
Purity (concentration of impurities)	99.95% [H_2O < 500 ppm, N_2 < 2 ppm, O_2 < 1 ppm, all others undetectable]	
Purity (concentration of impurities with optional high purity dryer)	ISO 14687:2019(E) Type I, Type II Grade D and SAE J-2719 Type I Grade L 99.9995% [H_2O < 5 ppm, N_2 < 2 ppm, O_2 < 1 ppm, all others undetectable]	
Start-up Time (from standby)	< 8 min	
Ramp-up Time (minimum to full load)	< 15 sec	
Ramp Rate (% of full-scale)	≤ 15% per sec	
Production Capacity Dynamic Range	10 to 100%	
POTABLE WATER REQUIREMENTS		
Consumption Rate at Intermittent Flow	705 l/h (186 gal/h)	1,100 l/h (282 gal/h)
Temperature	5 to 35°C (41 to 95°F)	
Pressure	2.7 to 4.8 barg	
Input Water Quality	Potable, subject to site water quality analysis	
Water Purification System (included)	Reverse Osmosis/Electrodeionization (RO/EDI)	

MODEL		MC250	MC500
ELECTRICAL SPECIFICATIONS			
Electrical Requirements		Medium voltage: 6.6 to 35 kV, three phase 50 Hz/60 Hz Low voltage, three phase required for balance of plant and ancillary equipment Backup, low voltage, three phase required for emergency heating for freeze protection	
Power Quality (medium voltage)		Total harmonic distortion: < 5%, power factor: > 0.9	
PHYSICAL CHARACTERISTICS			
Dimensions W x D x H	Power Supply Enclosure	6.1 m x 2.5 m x 2.6 m (20 ft x 8 ft x 8.5 ft)	6.1 m x 2.5 m x 2.6 m (20 ft x 8 ft x 8.5 ft)
	Electrolyser Enclosure[2]	12.2 m x 2.5 m x 3 m (40 ft x 8 ft x 9.9 ft)	12.2 m x 2.5 m x 3 m (40 ft x 8 ft x 9.9 ft)
Weight	Power Supply Enclosure	14,000 kg (31,000 lbs)	14,000 kg (31,000 lbs)
	Electrolyser Enclosure[3]	17,300 kg (38,000 lbs)	18,600 kg (41,000 lbs)
ENVIRONMENTAL CONSIDERATIONS – DO NOT FREEZE			
Standard Siting Location		Outdoor, pad mounted Flatness 35/25 per ACI-117-10 Bottom access for AC and DC electrical connections, water and drains	
Storage/Transport Temperature		5 to 60°C (41 to 140°F)	
Ambient Temperature		-20 to 40°C (-4 to 104°F)	
Altitude Range – Sea Level		1,000 m (3,281 ft)	
OPTIONS			
• Medium voltage input 4.16 to 6.6 kV • High ambient temperature -20 to 45°C (-4 to 113°F)	• Thermal Control System • Low ambient temperature -30 to 40°C (-22 to 104°F)	• High purity hydrogen dryer with dew point meter	